EXPERIMENTAL DESIGN AND STATISTICAL MODELING FOR EFFICIENT WIND TUNNEL TESTING

A THESIS SUBMITTED TO
THE GRADUATE SCHOOL OF NATURAL AND APPLIED SCIENCES
OF
MIDDLE EAST TECHNICAL UNIVERSITY

BY

ÖZGÜN SAVAŞ

IN PARTIAL FULFILLMENT OF THE REQUIREMENTS
FOR
THE DEGREE OF MASTER OF SCIENCE
IN
AEROSPACE ENGINEERING

SEPTEMBER 2019

Approval of the thesis:

EXPERIMENTAL DESIGN AND STATISTICAL MODELING FOR EFFICIENT WIND TUNNEL TESTING

submitted by **ÖZGÜN SAVAŞ** in partial fulfillment of the requirements for the degree of **Master of Science in Aerospace Engineering Department, Middle East Technical University** by,

Prof. Dr. Halil Kalıpçılar
Dean, Graduate School of **Natural and Applied Sciences** _____

Prof. Dr. İsmail Hakkı Tuncer
Head of Department, **Aerospace Engineering** _____

Assist. Prof. Dr. Ali Türker Kutay
Supervisor, **Aerospace Engineering, METU** _____

Examining Committee Members:

Prof. Dr. Oğuz Uzol
Aerospace Engineering, METU _____

Assist. Prof. Dr. Ali Türker Kutay
Aerospace Engineering, METU _____

Prof. Dr. Serkan Özgen
Aerospace Engineering, METU _____

Prof. Emer. Dr. Hüseyin Nafiz Alemdaroğlu
School of Civil Aviation, Atılım University _____

Assoc. Prof. Dr. İlkay Yavrucuk
Aerospace Engineering, METU _____

Date: 05.09.2019

I hereby declare that all information in this document has been obtained and presented in accordance with academic rules and ethical conduct. I also declare that, as required by these rules and conduct, I have fully cited and referenced all material and results that are not original to this work.

Name, Surname: Özgün Savaş

Signature :

ABSTRACT

EXPERIMENTAL DESIGN AND STATISTICAL MODELING FOR EFFICIENT WIND TUNNEL TESTING

Savaş, Özgün
M.S., Department of Aerospace Engineering
Supervisor: Assist. Prof. Dr. Ali Türker Kutay

September 2019, 62 pages

Wind tunnel testing is an essential procedure to measure the aerodynamic forces and moments on an air vehicle. In this thesis, a method is presented to perform such test in an efficient way. First, an experimental design process is carried out before the testing in order to cover the flight regime as fine as possible with the least possible number of tests. After the determination of the test matrix and conducting the wind-on tests, the modeling of the output data is the next step. On that matter, since the vehicle of interest is an agile missile which may fly at high angles of attack and in a relatively broader Mach regime, the aerodynamic data is highly nonlinear. Therefore, two nonlinear modeling techniques are presented and compared with each other. First technique is the widely used Artificial Neural Networks (ANN) and the second one is relatively lesser known but a powerful modeling algorithm Multivariate Adaptive Regression Splines (MARS). After the data is modeled using both approaches, their statistical metrics are compared and the models are integrated into a high fidelity 6DoF equations of motion model. Since all this effort is to improve the simulation accuracy and performance, 6DoF simulations are performed using several flight sce-

narios that cover the flight regime of the missile. Afterwards, obtained trajectories and flight parameters are compared. Finally, various flight conditions are produced and the models are evaluated in batch mode to see their performances in terms of computational speed.

Keywords: Design of experiments, Modeling and simulation, Flight simulations, Wind tunnel testing, Experimental aerodynamics, Multivariate Adaptive Regression Splines, Neural Networks, Data sampling

ÖZ

VERİMLİ BİR RÜZGÂR TÜNELİ TESTİ İÇİN DENEY TASARIMI VE İSTATİSTİKSEL MODELLEME YÖNTEMİ

Savaş, Özgün
Yüksek Lisans, Havacılık ve Uzay Mühendisliği Bölümü
Tez Yöneticisi: Dr. Öğr. Üyesi. Ali Türker Kutay

Eylül 2019 , 62 sayfa

Rüzgâr tüneli testleri, bir hava aracına etkiyen aerodinamik kuvvet ve momentleri ölçmede önemli bir kaynaktır. Bu tezde, rüzgâr tüneli testini verimli bir şekilde gerçekleştirmek için bir yöntem sunulmuştur. İlk olarak, hava aracının uçuş rejimini mümkün olan en az sayıda testle en iyi şekilde kapsayan bir test matrisi oluşturabilmek için deney tasarımı çalışması gerçekleştirilmiştir. Test matrisi belirlendikten ve bu matrise göre rüzgâr tüneli testleri icra edildikten sonraki adım veriyi modellemektir. Bu konuda da yüksek hücum açılarında ve geniş bir Mach sayısı aralığında uçabilen çevik bir füze incelendiğinden aerodinamik verinin yüksek oranda doğrusal olmayan bir karakter göstereceği öngörülmektedir. Bu nedenle, bu çalışmada iki farklı doğrusal olmayan veri modelleme yöntemi sunulup birbiriyle karşılaştırılmaktadır. İlk yöntem, sık kullanılan "Yapay Sinir Ağları" , ikinci yöntem ise görece daha az bilinen ama güçlü bir modelleme algoritması olan MARS'tır. Her iki yöntemle rüzgâr tüneli verisi modellendikten sonra, istatistiksel metrikleri karşılaştırılan modeller 6 serbestlik dereceli yüksek başarımlı benzetim ortamına eklenmektedir. Çalışmanın temel amacı, benzetim ortamının doğruluğunu ve başarımını artırmak olduğundan,

çevik füzenin uçuş rejimindeki birçok uçuş senaryosu simule edilip elde edilen yörüngeler ve uçuş parametreleri karşılaştırılmıştır. Son olarak, oluşturulan çok sayıda uçuş koşulu bu modellerde yığmalı şekilde çalıştırılıp yöntemlerin başarımları hesaplama zamanı açısından karşılaştırılmıştır.

Anahtar Kelimeler: Deney tasarımı, Modelleme ve simulasyon, Uçuş benzetimleri, Rüzgâr tüneli testleri, Deneysel aerodinamik, MARS, Yapay sinir ağları, Veri örnekleme

Dedicated to Mukaddes Savaş, my dear departed grandmother.

ACKNOWLEDGMENTS

I would like to express my greatest gratitude to my supervisor, Asst. Prof. Dr. Ali Türker Kutay, for his valuable guidance and constructive feedback during this thesis. His belief in the subject encouraged me to pursue further and expand the scope of the thesis.

I am grateful to my mother Özden and my sister Neşe for their endless love, patience and support throughout my life. Also, I would like to thank my beloved Gamze for all her love and support. It is an ultimate delight to witness the life together with you.

I would like to thank my former and current division chiefs and group coordinator Ümit Kutluay, Kenan Ünal and Osman Başoğlu respectively. Their invaluable guidance, insights, encouragements and criticism made a large contribution to this work. I need to express my sincere thanks to my colleagues Eren Topbaş, Hüseyin Deniz Karaca, Nabi Vefa Yavuztürk, Melih Koçak, Hakan Sargın and Hasan Başar Bolat for their help throughout this work. I thank Prof. Dr. İnci Batmaz for sharing valuable recommendations and feedbacks on issues regarding statistics.

In addition, I would like to thank my friend Ali Oğuz Yüksel for his help on LaTeXthat enabled a better writing process.

This thesis is supported by Defense Industries Research and Development Institute (SAGE) of The Scientific and Technological Research Council of Turkey (TUBITAK).

TABLE OF CONTENTS

LIST OF TABLES

TABLES

LIST OF FIGURES

FIGURES

LIST OF ABBREVIATIONS

ABBREVIATIONS

6DoF	Six Degree of Freedom Simulation Model
AIAA	American Institute of Aeronautics and Astronautics
ANN	Artificial Neural Networks
BF	Basis Functions
CFD	Computational Fluid Dynamics
deg	degrees, °
DoE	Design of Experiments
DoF	Degree of Freedom
FDS	Fin Deflection Set
Fr	Froude Number
GPS	Global Positioning System
GPU	Graphical Processing Unit
HLS	Hidden Layer Size
Hz	Hertz
INS	Inertial Navigation System
LHS	Latin Hypercube Sampling
Mach	Mach Number
MARS	Multivariate Adaptive Regression Splines
MDoE	Modern Design of Experiments
MSE	Mean Squared Error
NN	Neural Networks
OFAT	One-Factor-At-a-Time

Re	Reynolds Number
SSE	Sum of Squares due to Error
SSR	Sum of Squares due to Regression
SST	Total Sum of Squares
Str	Strouhal Number
UAV	Unmanned Aerial Vehicle
WT	Wind Tunnel

LIST OF SYMBOLS

SYMBOLS

α	Angle of attack
α_{tot}	Total angle of attack
β	Angle of sideslip
$C_x,\ CX$	Axial force coefficient along +x_b
$C_y,\ CY$	Side force coefficient along +y_b
$C_z,\ CZ$	Normal force coefficient along +z_b
$C_l,\ CLL$	Rolling moment coefficient around +x_b
$C_m,\ CM$	Pitching moment coefficient around +y_b
$C_n,\ CLN$	Yawing moment coefficient around +z_b
$^\circ$	degrees
δ_a	Aileron deflection angle
δ_e	Elevator deflection angle
δ_r	Rudder deflection angle
$\delta_{a,e,r}$	Aileron, elevator, rudder deflection angles (virtual controls)
δ_i	i'th control surface deflection angle (actual controls)
δ_{sm}	Deflection squeeze mode
ϕ	Roll angle (around $+x_b$)
θ	Pitch angle (around $+y_b$)
ψ	Yaw angle (around $+z_b$)
Ω	Stability axis rotation rate
ω	Angular rates
ν	Measurement error

M	Mach number
r^2	Coefficient of determination
x_b	x-axis in body coordinates (positive out of nose)
y_b	y-axis in body coordinates (positive out the right wing)
z_b	z-axis in body coordinates (positive below aircraft)

CHAPTER 1

INTRODUCTION

1.1 Aerodynamic Modeling

Aerodynamics studies the motion of air particularly around the solid objects when moving through it. Even though multi storey building engineers and ground vehicles designers make use of aerodynamics, most of the aerodynamicists deal with aircrafts.

Aerodynamics has an utmost importance in aircraft design. This is due to most of the flight characteristics of the aircraft depends on external geometry. Important features such as stability, flight performance, maneuever capability, range, speed, endurance partially determined by the aerodynamic design.

In addition, aerodynamic model has to be obtained before the flight in order to successfully control the aircraft. Whether the aircraft has a pilot on board or it is an unmanned aerial vehicle (UAV), aerodynamic modeling is important. Furthermore, to design an autopilot for each type, an advanced aerodynamic characteristics knowledge is essential.

1.1.1 Aerodynamics Database Generation

There are several methods for aerodynamic database generation. In the early stages of the projects semi-empirical methods are widely used due to their speed. However, as the project advances and the geometry is more or less become clear, computational fluid dynamics (CFD) analysis become necessary. Despite usually costly in computational time, CFD analyses provides advanced results of aircraft aerodynamics.

Afterwards, following the geometrical freeze, aerodynamic ground test, i.e wind tunnel tests are conducted. This tests will further enhance the aerodynamic database and also validates all of the analyses which have been performed so far. Finally, with performing real flight test and collecting that data, through some techniques such as system identification, the aerodynamic model can be upgraded.

Figure 1.1 shows the aforementioned progress of aerodynamic database development.

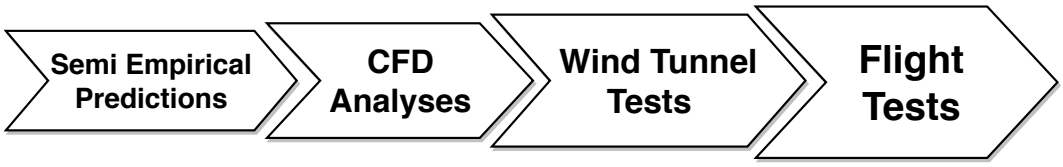

Figure 1.1: Aerodynamic Data Source Progress

1.1.2 Aircraft Properties

In this thesis, the aircraft of interest is an agile missile that travels through subsonic, transonic and supersonic Mach number regimes and controlled by four independent control surfaces, more specifically tail fins, and is capable of reaching high α and β values to be able to provide adequate turn performance. A generic geometrical representation of the aircraft of interest is shown in Figure 1.2.

This type of missiles operate within comparatively large flight envelope, broad Mach regime and reaches high α and β values, as in this case. This may result in a situation where the flight dynamics of the missile behave nonlinear with changing conditions. As a result, the design space is very large in terms of Mach number, α - β regions and control surface deflection angles. To cover that nonlinearity throughout the entire flight envelope, design of experiment and statistical modeling techniques that are suitable for this type of problem are investigated.

Having a large flight envelope in terms of every parameter is quite suitable for this study. Because, the challenges of each regime can be observed and the applicability of the method will be shown.

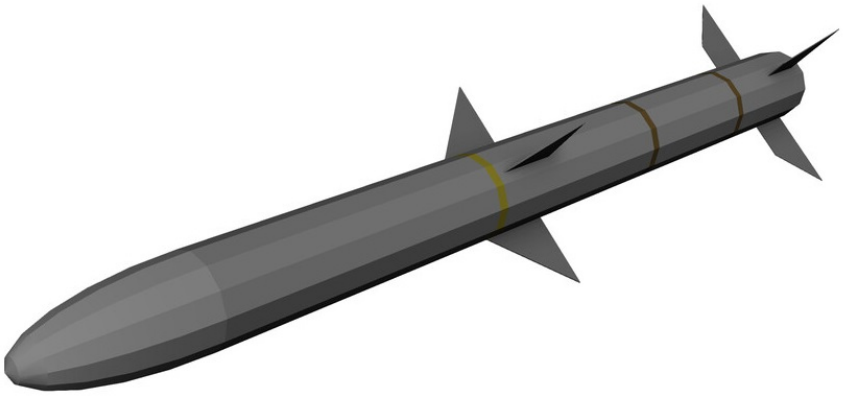

Figure 1.2: Generic Missile Geometry with Control Fins [1]

1.1.3 Aerodynamic Definitions

In this section, a summary of the aerodynamic coefficients, axes and equations of motion for 6DoF simulations is presented. Aerodynamic model consists of static and dynamic force and moment coefficients which are non-dimensional. The coefficients are defined with respect to the non-dimensional parameters derived based on dimensional quantities. The definition of an aerodynamic coefficient is given below;

$$C_i = C_i(\alpha, \beta, \delta, \frac{\Omega l}{V}, \frac{\dot{\Omega} l^2}{V^2}, \frac{\dot{V} l}{V^2}, Mach, Re, Fr, Str, ...) \tag{1.1}$$

$$\textit{where } i = x, y, z, l, m, n$$

Since mass and inertia of the missile are significantly larger than the surrounding air mass and inertia, fluid properties change slowly. Thereby, Froude Number effect is small. Moreover, because of the quasi-steady flow assumption, the flow adjusts instantaneously to changes. This result is an exception to Strouhal number effect [2]. The change in Reynolds number can also be neglected because it differs only slightly during the flight. Then, the Equation 1.1 becomes;

$$C_i = C_i(\alpha, \beta, \delta, \frac{\Omega l}{V}, \frac{\dot{\Omega} l^2}{V^2}, \frac{\dot{V} l}{V^2}, Mach) \tag{1.2}$$

For wind tunnel testing, the number of parameters is decreased to α, β, δ, Mach since it is not feasible, due to the requirements of special balance and sting mechanisms, for the dynamic components such as angular rates to be tested. For this reason, the coefficients that is to be calculated are static aerodynamic coefficients and does not incorporate the unsteady characteristics of the flow. Then, the Equation 1.2 reached its final form as follows;

$$C_i = C_i(\alpha, \beta, \delta, Mach) \tag{1.3}$$

The axis system that is used to define the aerodynamic coefficients and equations of motion is presented in Figure 1.3. The center of gravity of aircraft, "O", is the origin of both the stability and body axes. Body axis is defined as,

- Positive O_{xb} axis forward and aligned with the nose of the vehicle
- Positive O_{yb} axis points out the right wing
- Positive O_{zb} axis is directed through the downside which forms a right hand rule with x_b and y_b.

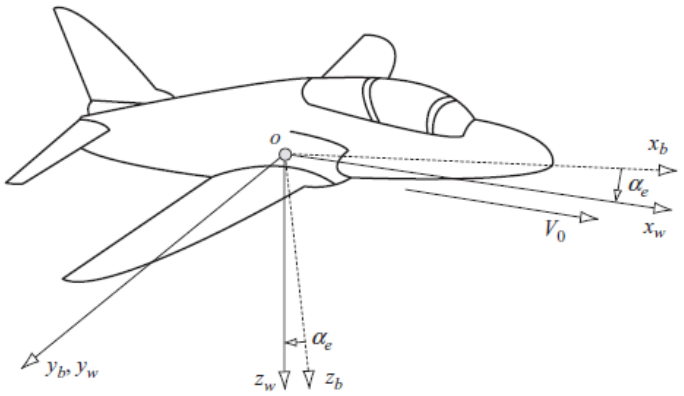

Figure 1.3: Aircraft Body and Stability Axis [3]

Table 1.1: Aerodynamic Forces and Moments

Coefficient	**Explanation**
C_x	axial force coefficient along $+x_b$
C_y	side force coefficient along $+y_b$
C_z	normal force coefficient along $+z_b$
C_l	rolling moment coefficient around $+x_b$
C_m	pitching moment coefficient around $+y_b$
C_n	yawing moment coefficient around $+z_b$

To simulate the agile missile, a 6DoF simulation model is to be built. In 6DoF model, the body assumed to be rigid, an assumption that eliminates the need to consider the interaction between individual elements of the missile [2]. Other than the rigid body motion assumption, the second simplification for 6DoF simulation is that the location of center of mass is coincident with the center of gravity. Effects due to structural deformations and relative motion of control surfaces during flight are assumed to be negligible. Also, the effect of the Earth's rotation is neglected due to considerable short flight time. With the simplification stated above, the governing equations for vehicle motion can be explained by Newton's 2^{nd} law;

$$\vec{F} = \frac{d}{dt}(m\vec{V}), \quad \vec{M} = \frac{d}{dt}(I\vec{\omega}) \tag{1.4}$$

The matrix representations of $\vec{F}$, $\vec{V}$, $\vec{M}$, I and $\vec{\omega}$ are given in Equation 1.5;

$$\vec{F} = \begin{bmatrix} F_x \\ F_y \\ F_z \end{bmatrix} \vec{V} = \begin{bmatrix} u \\ v \\ w \end{bmatrix} \vec{M} = \begin{bmatrix} M_x \\ M_y \\ M_z \end{bmatrix} I = \begin{bmatrix} I_x & -I_{xy} & -I_{xz} \\ -I_{xy} & I_y & -I_{yz} \\ -I_{xz} & -I_{yz} & I_z \end{bmatrix} \vec{\omega} = \begin{bmatrix} p \\ q \\ r \end{bmatrix} \tag{1.5}$$

In Figure 1.4, tail fin layout of the missile is given. As can be seen a cruciform tail fin layout is considered. When looking from behind, the fin on the top right is characterized as first and the numbering continued in clockwise direction.

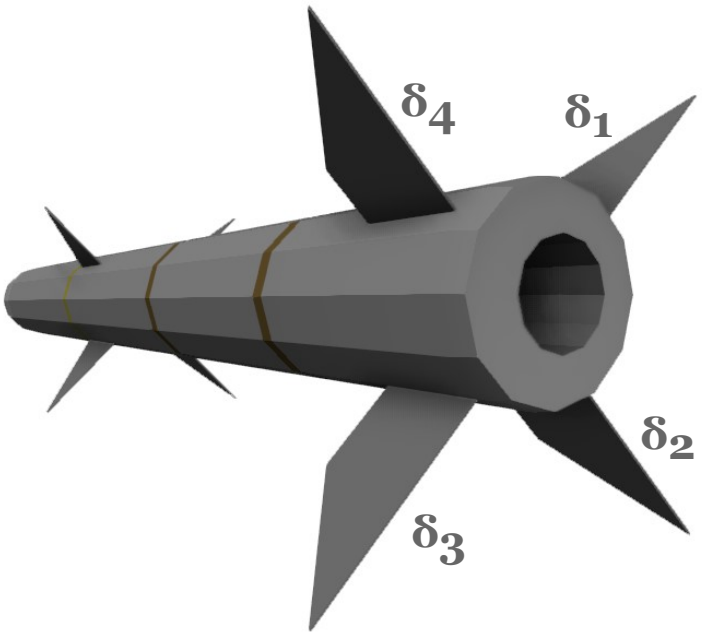

Figure 1.4: Tail Fin Layout of a Generic Missile Geometry [1]

Unlike an airplane, in most of the missiles, there is a concept called actual and virtual controls. In a conventional airplane; aileron controls roll motion, elevator control pitch motion and rudder controls the yaw motion. These are the three rotational degrees of freedom and considered virtual controls in missiles. The reason is that there is no dedicated control surface for each of that motions. Instead, by utilizing four tail fins independently, control authority for each axis is constituted. From the hinge line, the fins can rotate to either direction. Clockwise rotation of the leading edge is identified as a positive deflection for every fin. Using that convention, virtual controls can be derived from actual controls as in Equation 1.6. In addition, in Table 1.2, a summary of the conversion is stated.

$$\begin{aligned} \delta_a &= \frac{\delta_1 + \delta_2 + \delta_3 + \delta_4}{4} \\ \delta_e &= \frac{\delta_1 + \delta_2 - \delta_3 - \delta_4}{4} \\ \delta_r &= \frac{\delta_1 - \delta_2 - \delta_3 + \delta_4}{4} \end{aligned} \tag{1.6}$$

Table 1.2: Conversion Between Actual and Virtual Fin Deflections

Virtual Control	**Resultant Motion**	**Conversion Relation**
Aileron	Roll (ϕ)	$(+,+,+,+)$
Elevator	Pitch (θ)	$(+,+,-,-)$
Rudder	Yaw (ψ)	$(+,-,-,+)$

After the definition of virtual and actual controls, there is a need to define another virtual control called deflection squeeze mode, or δ_{sm}. Since there are three virtual and four actual controls, there may be some undesirable control couplings that reduce the control authority. To overcome that and minimize the control couplings in an autopilot design process, a new virtual parameter δ_{sm} is introduced in Equation 1.7 and forced to be around zero within a predefined tolerance level [4].

$$\delta_{sm} = \frac{\delta_1 - \delta_2 + \delta_3 - \delta_4}{4} \tag{1.7}$$

As explained earlier, for a single control input, there has to be four different fin deflection angles is to be determined. However, there are some boundaries for each and every parameter. Therefore, to keep the deflection angles reasonable within those limits, mathematical norm of the angles are calculated as in Equation 1.8. After that, norm is set to be between the respective boundaries for every flight condition as a design constraint.

$$norm = \sqrt{(\delta_1)^2 + (\delta_2)^2 + (\delta_3)^2 + (\delta_4)^2} \tag{1.8}$$

1.1.4 Simulation Model

Flight simulation models are quite important in aircraft system design. They offer plenty of benefits throughout the design and test processes. They probably will gather more interest in time now that the model based design has an increased importance in aerospace industry.

There are several type of simulation models depending on complexity. In this ap-

plication, the model of interest is a six degree of freedom (6DoF) simulation model consisting of 3 translation degrees of freedom (DoF) and 3 rotational DoF. Using them one can design and integrate any subsystems, analyze the trajectory, orientation, design subsystems, perform optimizations etc. 6DoF model includes complex subsystems such as guidance and autopilot, navigation, fin actuation system, atmosphere, wind and gust models, rocket propulsion and last but not least an aerodynamic model.

Simple representation of the flight simulation model is illustrated in Figure 1.5.

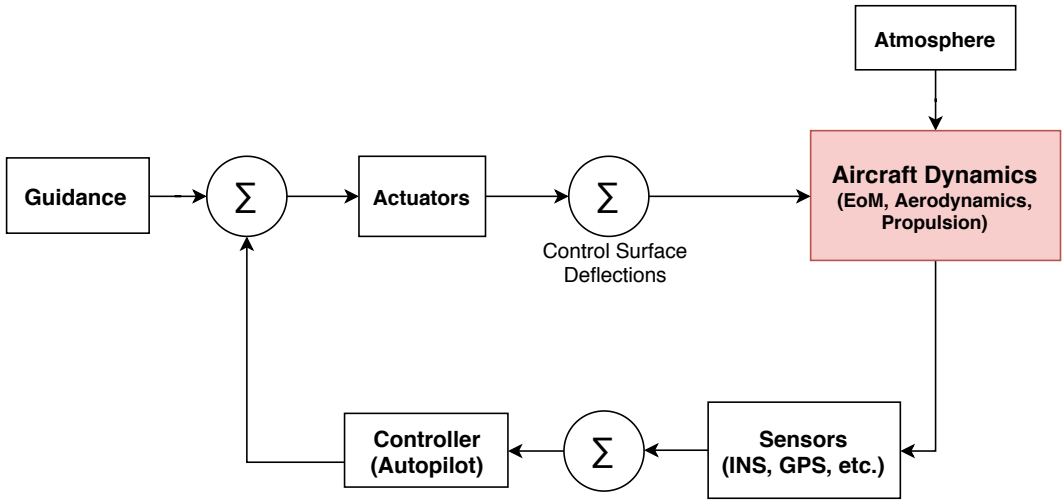

Figure 1.5: Flight Simulation Model Block Diagram

To perform simulations that are similar to the real world dynamics, the subsystems have to be accurate so that the overall model performs well. The subsystem that is to be improved in this study is the aerodynamic model of the aircraft.

1.2 Motivation and Proposed Methodology

Wind tunnel testing is extensively used in the aerodynamic characteristic determination of solid bodies, mostly air vehicles. Even though computational fluid dynamics (CFD) tools are becoming more advanced day by day, their results are not completely accurate and the need of real world testing remains necessary to validate its results.

However, unfortunately wind tunnels are quite expensive since it is an exhausting task from producing the perfectly scaled model, setting the correct pressure and turbulence intensity, wind-on testing, data collection and post processing.

In this thesis, aerodynamic database of an aircraft is to be obtained using wind tunnel testing in an efficient way without compromising data accuracy. The aim is to do it in such a way that it is accurate, as less expensive as possible and the final product does not require abundant computational resources. Because, wind tunnel testing is quite expensive and by using statistics and nonlinear modeling, huge amounts of expenses may be saved [5].

In Figure 1.6, proposed methodology can be seen as a flowchart.

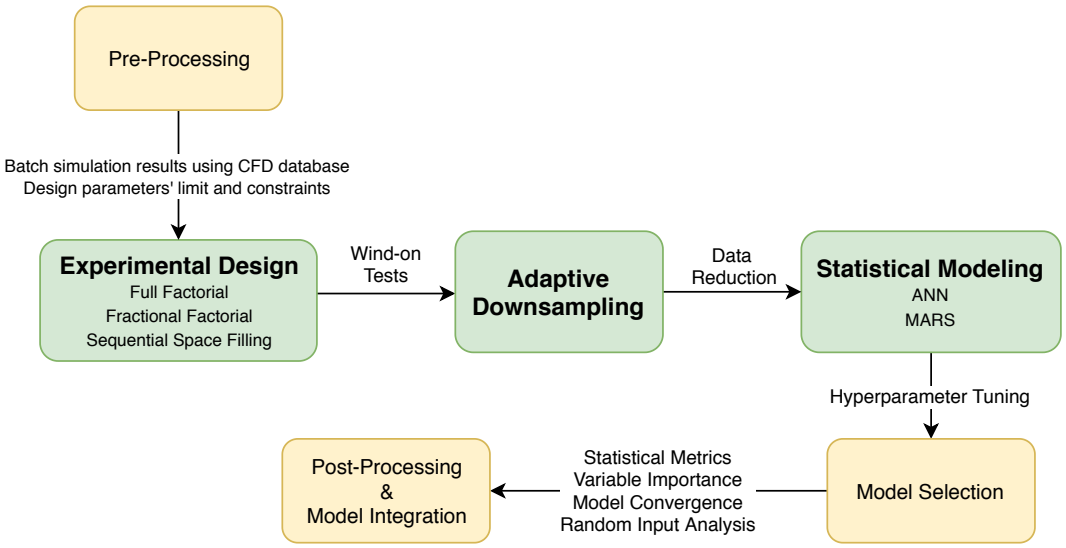

Figure 1.6: Flowchart of the Proposed Procedure

1.3 Contributions and Novelties

In today's world, most of the breakthroughs are made through blending the scientific disciplines. This study inspired from that fact and brought together the cutting edge technologies from computer science and statistics into an aerospace problem.

Following will be the most important contributions of this study and they may help be to the ones that has the same challenge:

- Propose a method to perform cost effective wind tunnel campaigns
- Shows how to evaluate the experimental design in statistical metrics along with the technical graphs on scenario coverage
- Demonstrates how to perform model assessment like variable importance, model convergence, overfitting prevention and random input analysis

1.4 Literature Review

Only few studies have been found on this topic. The reason behind it may be the know-how sharing issue since most of the applications are on defense industry. In addition to that, even though neural networks are known for years, to apply that methodology in such a data rich field is dependent on the recent drastic improvements on computational resources especially on graphical processing units (GPU).

Early work on modern design of experiment (MDoE) applications on wind tunnel test results are published by DeLoach, 1998 [6]. The implications from the paper is positive towards the use of MDoE in wind tunnel test matrix determination.

Application of neural networks on the wind tunnel test result modeling is previously considered. Integration of several linear regression methods into two different neural network algorithms, namely back propagation networks and radial basis function networks, is given [7]. It suggests that artificial neural networks are capable of modeling the nonlinear behaviour of the wind tunnel data.

Apart from wind tunnel aerodynamic modeling, space filling algorithms for various applications are investigated.

Latin Hypercube Sampling (LHS) is a method of statistical random sample generation for high dimensional cases. Sequential schemes with LHS have several advantages on undersampling and oversampling compared to one shot LHS [8].

It has been suggested that Monte Carlo based highly efficient sequential space filling algorithms are quite suitable for experimental design of multivariate problems [9].

Consequently, considering the prior work on the subject, design of experiments is a

such a suitable and effective application to the problem. Apart from that, nonlinear modeling techniques and artificial neural networks are applicable on the modeling part.

CHAPTER 2

METHODOLOGY

2.1 Design of Experiment

Before launching a wind tunnel test campaign, test matrix should be prepared with the utmost consideration. For that purpose, there is a concept called Design of Experiments (DoE). There are different approaches to DoE, but the main breakdown is one-factor-at-a-time (OFAT) or the methods that consider multiple factors simultaneously. In this thesis, the latter will be applied and its advantages will be stated.

For the missiles, the typical parameters for design of experiment and mathematical modeling are angle of attack (α), angle of sideslip (β), Mach number, and control surface deflections (δ_i) . Those are the design parameters or factors that will be simultaneously considered when designing the wind tunnel experiment. Control surface deflections can also become an independent variable thanks to the wind tunnel model that has a motorized fin deflection adjuster. That automatic fin deflection system saves a lot of wind tunnel time and enables more tests to be performed.

Moreover, wind tunnel testing is usually conducted using traverses, sometimes called sweeps or polars. That means, once the flow Mach number, sideslip angle and the fin deflections are set, aircraft starts from one position and be continuously rotated vertically through the flow while recording the aerodynamic data using a robotic arm. That process is called an angle of attack sweep and includes a lot of data point in the respective testing conditions.

Considering all that, the absolute aim is to cover the entire flight regime of the missile with the least number of tests since the tests are quite costly and time-consuming.

2.1.1 Full Factorial Designs

In experimental design, full factorial designs take all the possible combinations into account by fully crossing the factors with each other. In other words, when there is more than one factor with possible discrete values, one can design such an experiment that cross every factor and their value with each other to investigate the interactions of the parameters.

However, this type of experiment will require a lot of experimental effort when dealing multiple factors with large value range. In Figure 2.1, a full factorial experimental design on three parameters is shown.

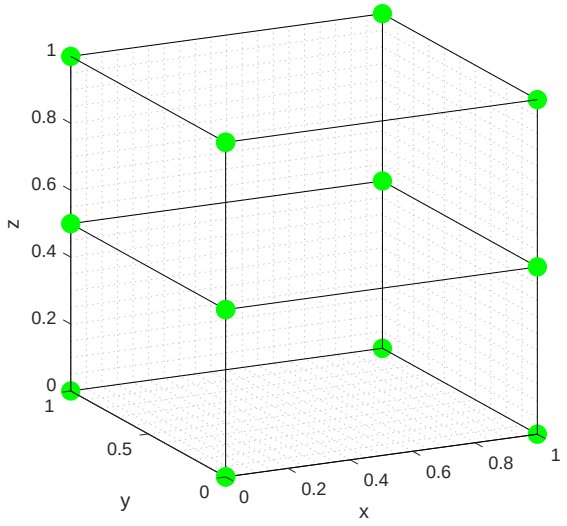

Figure 2.1: Full Factorial Experimental Design

2.1.2 Fractional Factorial Designs

Unlike the full factorial designs, fractional factorial designs consist of the subset of the all possible combinations. That subset is determined using prior knowledge of interactions between the factors. That way, the experimental effort is reduced since taking the fraction of the whole set prevents redundant tests to be performed. In Figure 2.2, a fractional factorial experimental design on the previous three parameters is shown.

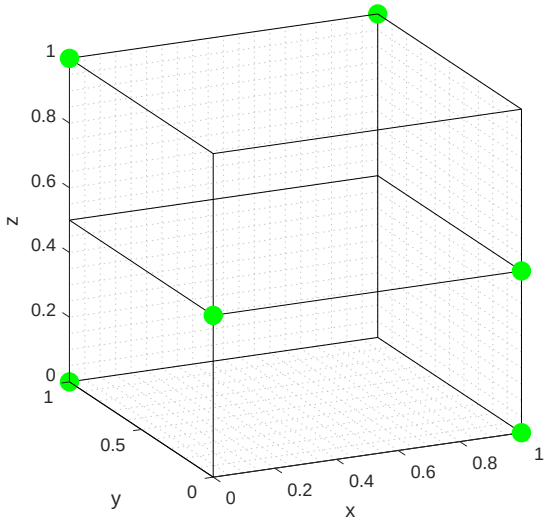

Figure 2.2: Fractional Factorial Experimental Design

2.1.3 Sequential Space Filling

This method is called either sequential or incremental space filling algorithm. Both names intend to indicate the space filling algorithm takes place through some stages or phases. Figure 2.4 shows the one stage space filling design for the previous three parameter design space.

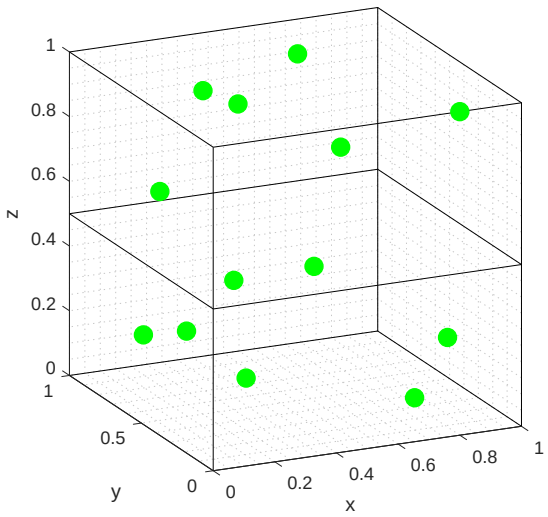

Figure 2.3: Space Filling Experimental Design

The wind tunnel test campaigns are usually performed in different phases which may have different aims and utilize different test matrices that cover a space with a number of parameters. Different approaches can be taken which may include a uniform matrix of test points that cover a design space or randomly generated and optimized points that cover the design space with combinations of parameters. The aim is to generate enough data from wind tunnel testing that covers the entire space while including a combination of parameters at a level to achieve a mathematical model that predicts dependent parameters with accuracy during simulations.

For the case of this work, firstly a uniform test matrix with OFAT approach is designed to understand the aerodynamic characteristics of a missile with a limited number of test points. The reason behind this is to validate the current aerodynamic database which is generated using CFD. The rest of the test points are inserted to cover the entire design space with different combinations of parameters in two phases. Therefore, a specific DoE approach named space filling design methodology seems appropriate for this problem.

Space filling designs aim to place the new points in a uniform manner while maximizing the distance between each test point in the design space. In addition to that, with space filling, different set of points can be generated consecutively which makes its use reasonable on a multi-phased wind tunnel test campaigns. Since the test campaign in this case have a number of phases, while designing the experiment of the new phases, the test conditions that were performed in the previous phases are also considered. Incremental or sequential approach of space filling helps add test points onto an existing set of points considering the distances between each point combination in the multi-dimensional space.

Figure 2.4 represents a sample DoE result. The blue dots are Phase 1 test conditions that are placed in uniform manner, which happens to be an initial test points for the upcoming sequence of Phase 2 that are illustrated by the red dots. The green dots represent the Phase 3 test conditions which are generated using both the blue and the red ones as initial test points. That sequential approach may continue as much as desired.

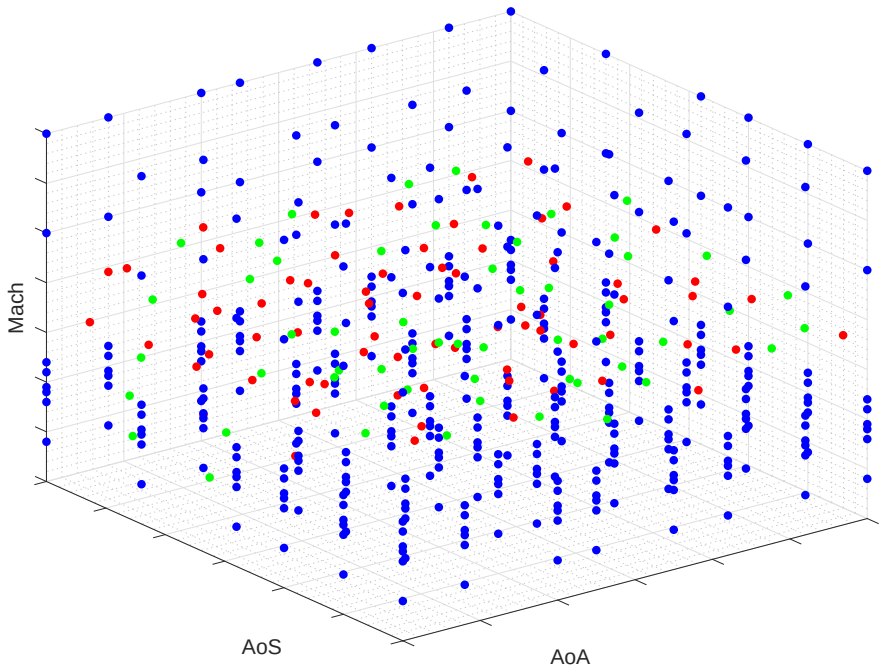

Figure 2.4: Sequential Space Filling Example

2.2 Adaptive Downsampling

Upon completion of the experimental design and the wind-on tests, resultant data can be obtained. Usually for a wind tunnel test, despite depending on the data acquisition ability and agreement, entire data set is really large. That mostly depends on the data acquisition frequency and most of the time it is abundantly frequent just because the equipment can provide as much.

However, that frequent of a data may cause some some problems. That's why the raw aerodynamic data should be resampled into a somewhat smaller data set. While doing the resampling, or downsampling in this case, data cannot be arbitrarily omitted. The purpose is to get rid of the redundant measurements in each traverse. Therefore, downsampling shall be performed in an adaptive manner for each traverse.

To do that, an algorithm is utilized and run for each traverse to perform downsampling. The procedure of the algorithm is as follows;

- Sort the data with respect to the independent variable
- Define a tolerance value for triangle area
- Starting from the first three data points draw a triangle connecting each points
- Calculate the enclosed triangle area and check if it exceeds the tolerance
- If the tolerance value is exceeded keep the point, if not eliminate the data point in the middle
- Continue with the successive data points

In addition to increase in efficiency by eliminating redundant data points, adaptive downsampling enables automatic data filtering and smoothing, which is also useful for modeling.

In Figure 2.5, downsampling of a random traverse is shown. Original data is downsampled from 138 data points into 43, which is roughly 30%.

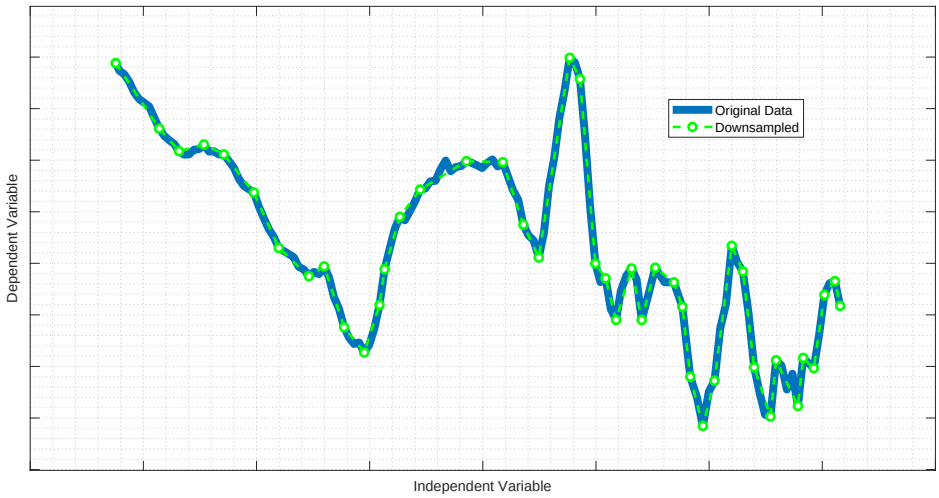

Figure 2.5: Downsampling Example

2.3 Statistical Modeling

The modeling of the aerodynamic coefficients based on the measured aerodynamic parameters is the next step. After finalizing the test matrix by DoE, the wind tunnel tests will be carried out on those conditions. Afterwards, the modeling takes place. Accuracy of modeling the aerodynamic properties using the wind tunnel data is very important since the model performance solely affect the simulation accuracy. The aerodynamic models that will be obtained at the end of modeling study are integrated into six-degree-of-freedom (6DoF) equations of motion model of the missile. Models with higher complexity and accuracy would lead to higher simulation accuracy, obviously. However, the model which will be used during simulations needs also be able to perform in a reasonable speed as well. That emerges a trade-off between accuracy and performance.

There are several studies in the past that suggest a number of methods to model the aerodynamic coefficients. The simplest method is using linear interpolation technique on multiple dimensions over the data. The dimensions for the case of this study are Mach number, α, β and control surface deflections. This approach requires OFAT type of experimental design and includes shortcomings of the methodology. There are studies on more complex methods to model the data collected from testing with DoE. The more complex methods are able to model interactions between the parameters. The outcome of the models is linear or nonlinear functions depending on the methods. It is possible to categorize the modeling techniques as parametric and non-parametric classes. The techniques that are presented above have advantages and disadvantages. Obviously, the linear interpolation technique has a disadvantage of not modeling interaction of parameters. However, it is the easiest modeling technique to understand the physical phenomenon at hand. The parametric modeling technique has the ability to model interactions in the aerodynamic data; yet, the technique is not able to model the nonlinearities that occur in the physical plane. Still, the physical meaning of the model is understandable through the order of the parameters. Parametric modeling techniques such as stepwise regression and least squares or orthogonal modeling techniques are widely used in aerospace field to model aerodynamic coefficients [3]. However, for modeling of nonlinear data, this class of techniques is not very

effective due to the nature of the mathematics behind it. Non-parametric techniques are able to model nonlinearities with success. But, the nature of the non-parametric model allows the possibility of overfitting and the resulted model functions can be unpredictable. The physical understanding of the resulted model is much harder to understand and control. Parametric techniques are relatively easy to understand and generally protected against "overfitting" since they are subjected to statistical testing such as normality of residuals, goodness-of-fit etc.

2.3.1 Overfitting and Selection Bias

Overfitting takes place when the model is redundantly complex, and the result has low predictive performance. It happens due to the methodology's excessive effort to model every behavior of the data. Overfitting usually occurs when there are many predictors or parameters. In order to visualize the underfitting and overfitting concepts Figure 5 is presented. The function that is underfitting can be seen in red color which has a linear fit that barely represents the data. Function that is overfitting can be seen in blue color which passes through nearly all points and has nice statistical performance, yet it is so concentrated on the existing data that the overfitting function does not work well in the predictive sense. A good fit is expected to look like the green line as given in the figure.

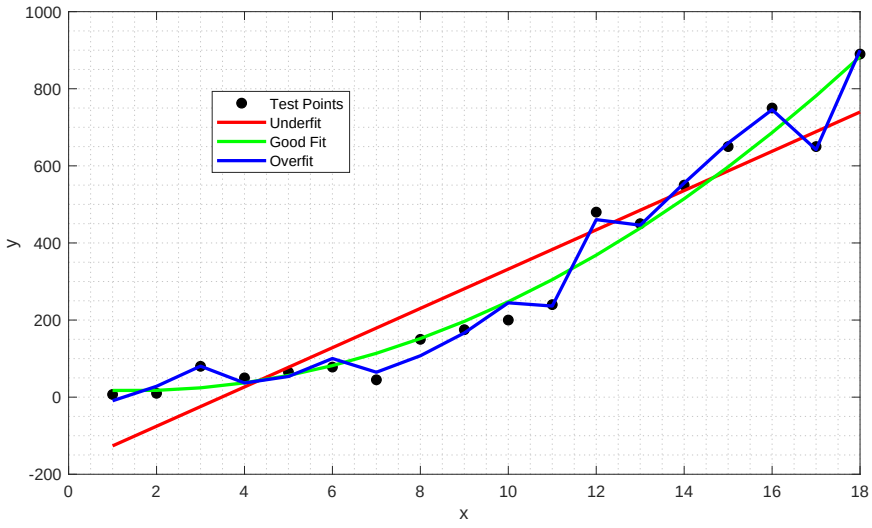

Figure 2.6: Underfitting and Overfitting Visualization

On the other hand, there is one more undesirable phenomenon called selection bias. Selection bias is an experimental error introduced when the selected data does not represent the entire data population. When modeling, input data is to be partitioned in a random manner. If one of those partitions happen to include selection bias, that cause some adverse effects on modeling. To prevent selection bias, cross validation technique can be applied.

2.3.2 Cross Validation

Artificial neural networks and MARS starts modeling the data with partitioning the initial data into two subgroups, train and test data sets. Both algorithms use training, or sometimes called learning, data set for analyzing and exploring the trends, effects and the interactions. After the training is completed, the resultant model is to be tested on the remaining of the data which happens to be the test data set, sometimes called hold out sample. That way, the algorithm knows how good the model performance is at that instant.

The process of partitioning the data is important and it must be carried out carefully. Most of the time, it depends on random selection. But, the selection of the test sample must be performed without compromising the remaining data. Because, the model will learn the patterns from that remaining training data set.

Also, sometimes that selection may cause to some errors if the selected subset happens to be misleading. That concept is called selection bias and should be avoided.

To prevent all that from happening, popular solution is performing a cross validation. Cross validation is the process of consecutively changing the test sample data in the population. Total number of consecutive sample selection determines the k value in k-fold cross validation. For instance, if the partitioning will be repeated 5 times, there happens to be 5 different test samples and that constitutes 5-fold cross validation modeling as in Figure 2.7.

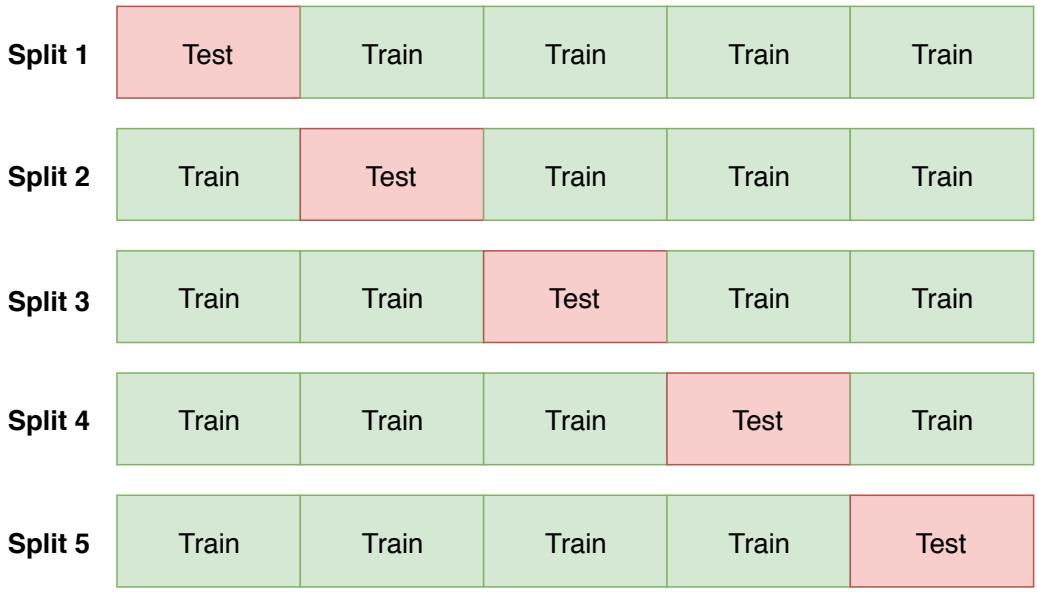

Figure 2.7: k-fold Cross Validation Scheme

2.3.3 Common Remarks on Selected Methods

For the class of non-parametric techniques, the most common technique is the artificial neural networks (ANN) technique which is also widely used in aerospace with success [7], [10]. The technique is nonlinear and non-parametric in nature. As a result, the statistical test metrics, such as goodness-of-fit, cannot be used to evaluate the models. The non-parametric techniques have great potential to model nonlinearities in data, however they are also quite perceptive to "overfitting". To overcome that, there are some techniques and cross validation is the outstanding one.

For the modeling problem of this study, the data to be modeled is highly nonlinear since the vehicle passes through a vast region of Mach number and flight angles. Also, the control surface deflections cover a good amount of area in experimental design space. In this case, it is highly unlikely to acquire a model of high accuracy with linear parametric modeling techniques. The studies on non-parametric modeling method ANN revealed that the test data can be modeled with high accuracy with a penalty of very long functions which has an impact on the simulation time. Since the aim is to produce a model function to be used in simulations, the search for a new type of non-parametric modeling technique with simpler model functions is done.

The Multivariate Adaptive Regression Splines (MARS) technique is proposed and evaluated to be a contender to ANN while decreasing calculation time during the simulations.

2.3.4 Artificial Neural Networks (ANN)

Artificial Neural Networks (ANN) is a computing technique inspired by human brain and nervous system as a network of units called neurons. It is estimated that the human brain have approximately 10 billion neurons each having connection with 10000 others. The mathematical model view of a neuron as a basic building block of ANN can be shown as in Figure 6. ANN works with layers such as input layer, output layer and optional hidden layers. Input layer presents the patterns of the data and through hidden layers, where the data processing is performed, input layer makes a connection to the output layer. [11]

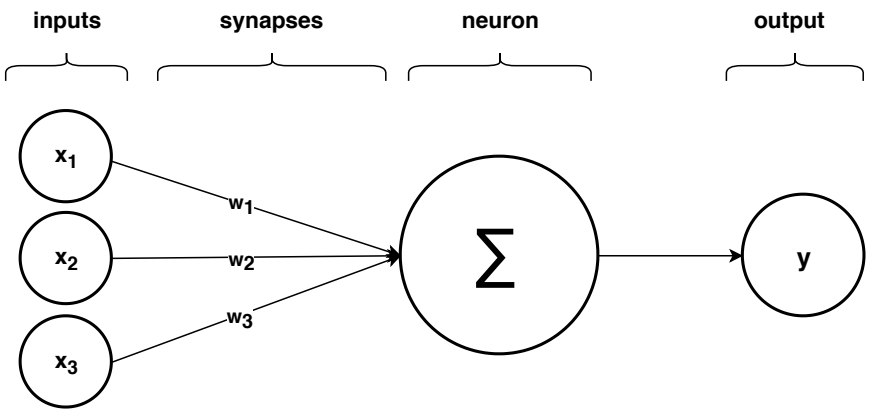

Figure 2.8: Simple Artificial Neural Network - Perceptron

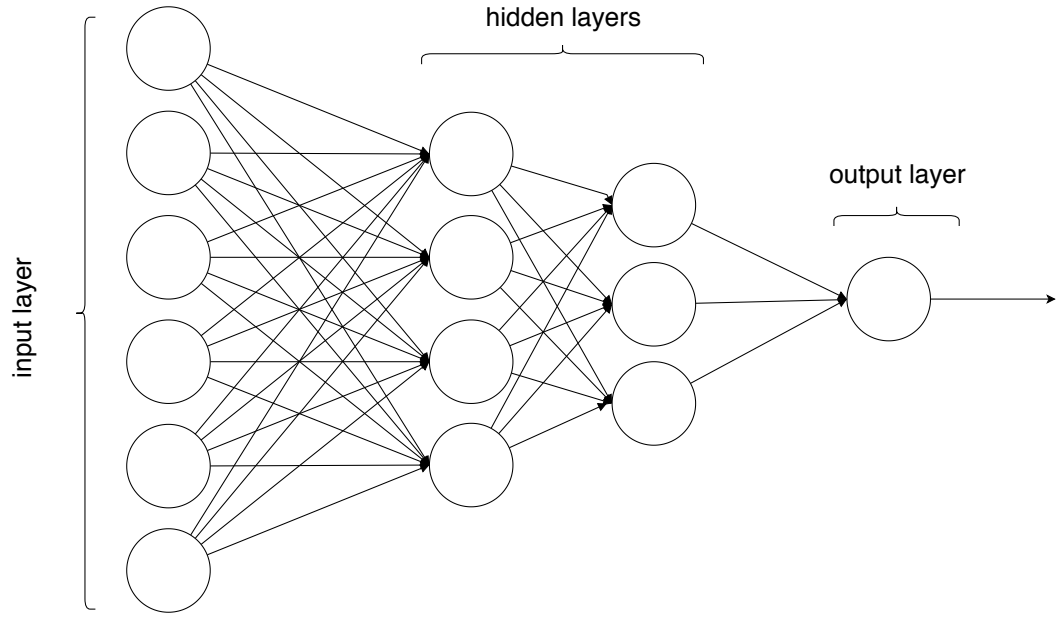

Figure 2.9: Multi-Layer Artificial Neural Network

There are a number of different architectures of ANN to propose solution to different type of problems. Since this study is about curve fitting to wind tunnel test data, curve fitting aspect of ANN is considered. The idea behind curve fitting is to select the suitable parameters that minimize the error over the set of data. ANN is a widely used nonlinear modeling technique that relates the output(s) with the input(s) on curve fitting problems. The most successful applications in curve fitting and modeling of neural networks are multi-layer networks. This type of networks simply accept the input values and successive layers of nodes. The outputs of neurons in a layer are inputs to neurons in the next layer. The last layer is called the output layer. Layers between the input and output layers are called as hidden layers

ANN works well on large set of data with nonlinear relationships. Therefore, it is appropriate to use ANN when modeling large and nonlinear aerodynamic datasets.

2.3.5 Multivariate Adaptive Regression Splines (MARS)

Multivariate Adaptive Regression Splines (MARS) is an adaptive procedure for regression which is introduced by Jerome H. Friedman, [12] and trademarked to Salford Systems.

The technique is well suited for problems with multiple inputs. It can be viewed as a generalization of stepwise linear regression using splines instead of a whole function. Technique works in two parts which are forward selection and backward elimination [13].

MARS technique uses expansions in piecewise linear basis functions (BF) of the form like $(x-t)_+$ and $(t-x)_+$ where "+" means positive part. The formulation is given in Equation 2.1.

$$(x-t)_+ = \begin{cases} x-t, & \text{if } x > t \\ 0, & \text{otherwise} \end{cases} \qquad (t-x)_+ = \begin{cases} t-x, & \text{if } x < t \\ 0, & \text{otherwise} \end{cases} \tag{2.1}$$

where x resembles the value of the independent variable and t resembles the position of the knot. An example for the basis functions is given in Figure 2.10 for t value of 0.5.

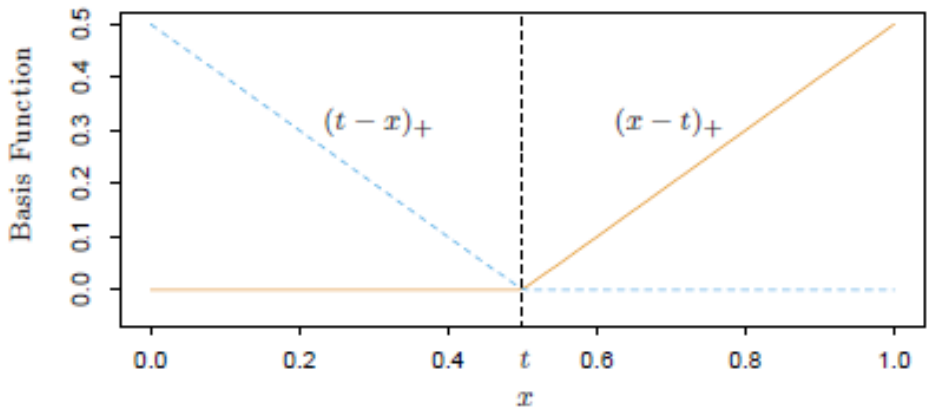

Figure 2.10: Example of Basis Functions [13]

The final model is constructed with a number of basis functions, Each BF piecewise linear, with a knot at the value t which can be defined as linear splines. The two functions are defined as reflected pairs. The technique forms reflected pairs for each input X_J at each value of $x_i J$. The collection of the basis functions define the function set C as in Equation 2.2.

$$C = \{(X_j * t)_+, /(t - X_j)_+\} \qquad t \in \{x_{1j}, x_{2j}, ..., x_{nj}\} \tag{2.2}$$

where j = 1, 2, 3, ..., p

where N resembles the number of data points and p resembles the number of inputs. As can be deduced from Equation 2.2, it is possible to generate (2 x N x p) BFs. The model building strategy is similar to stepwise regression. However, the functions in the set C are used in place of the original variables. The model form is presented in Equation 2.3.

$$f(x) = \beta_0 + \sum_{m=1}^{M} \beta_m h_m(X) \tag{2.3}$$

where $h_m(X)$ is a multiplication of two or more functions from set C. The procedure is very similar to least-squares regression technique. The forward selection part of the technique is illustrated in Figure 2.11, with first three steps. The left side shows the functions that are currently in the model while the right side covers the function pool that the selections will be from. At each state, all products in the pool are evaluated and the product that decreases the residual error the most is added into the current model.

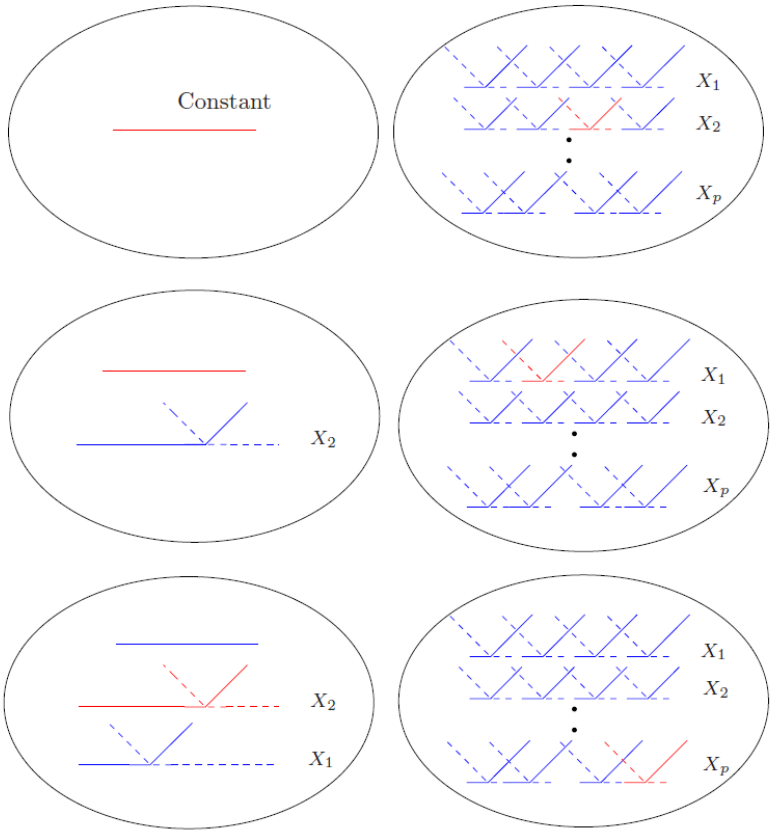

Figure 2.11: Forward Selection Part of Technique [13]

At the end of the forward selection, the acquired model is very large and inclined to overfitting. The backward elimination procedure is applied to remove the candidates which increase the residual error at the smallest amount until the final model is achieved.

CHAPTER 3

RESULTS AND DISCUSSION

In this chapter, result of the experimental design procedure, adaptive downsampling methodology and the statistical modeling process will be presented through various graphs and discussed.

3.1 Design of Experiment Results

This section will concentrate on the DoE results and show the flight scenario coverage of the design along with the performance graph on each parameter generated utilizing parallel coordinates chart.

3.1.1 Scenario Coverage

Prior to the wind tunnel testing, the simulation model was constructed with aerodynamic database generated using CFD. Using that model, a pool of simulation trajectories containing hundreds of flight scenarios were run and the results are saved for the further use. Analyzing that results can give not an overall but quite a meaningful insight about the aircraft and its behaviour. An overall understanding is only possible with real flight tests with every possible flight scenarios.

After the simulation results of the flight scenarios are obtained, the approach is to plot the relevant output together in the same figure in order to see the distribution of the flight parameters such as α, β and the actual and virtual fin deflection angles. Those parameters are to be plotted with respect to Mach number to see at which flow regime the parameters occur.

3.1.1.1 Flow Parameters

In Figures 3.1 & 3.2, scenario coverage of α and β are shown, respectively. Black lines represents the batch simulation results and the red lines are the DoE points for each parameter. In Figure 3.3, α and β results are given with respect to each other rather than Mach number.

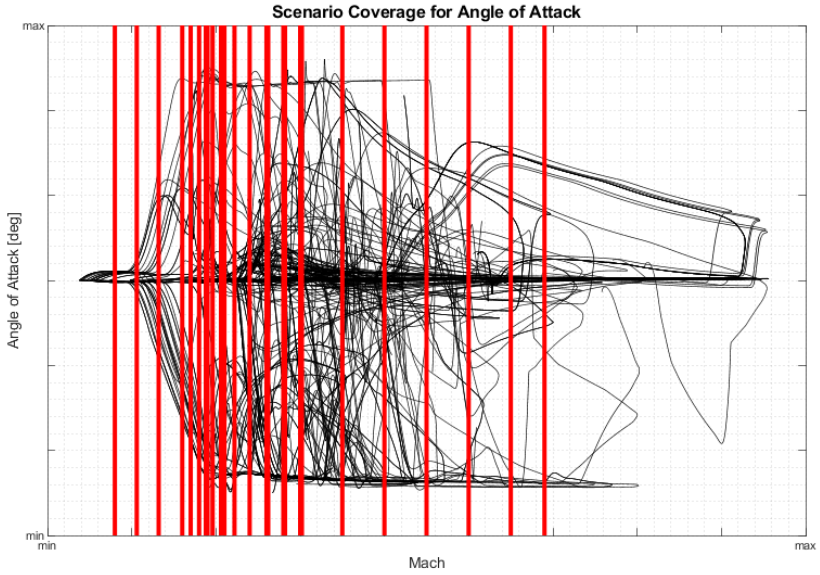

Figure 3.1: Scenario Coverage in Angle of Attack

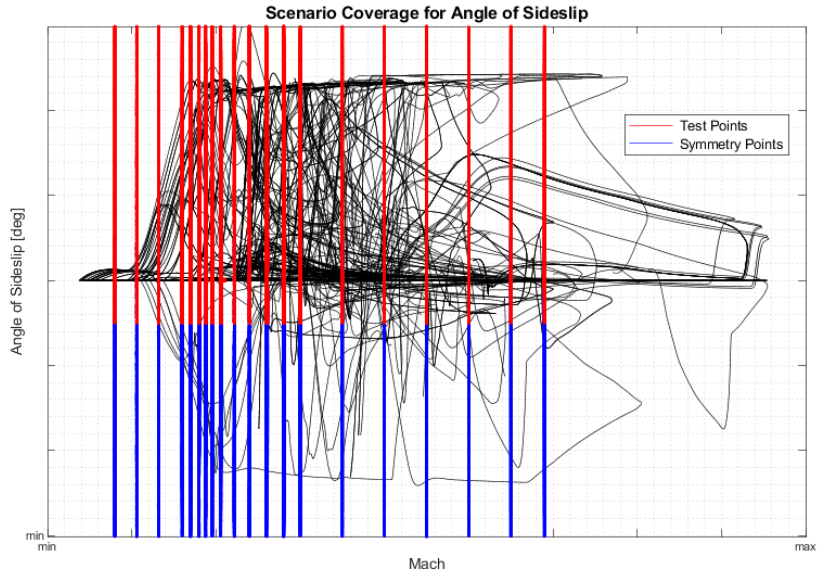

Figure 3.2: Scenario Coverage in Angle of Sideslip

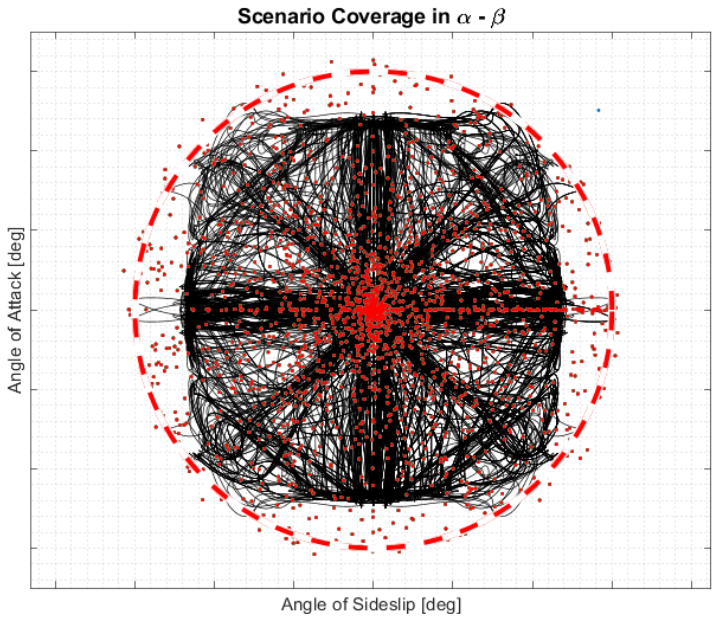

Figure 3.3: Scenario Coverage in α - β

Total angle of attack, α_{tot}, is the combination of angle of attack and angle of sideslip. It is meaningful when considering manuevers along both axes. α_{tot} is calculated as in Equation 3.1.

$$\alpha_{tot} = \cos^{-1}(\cos\alpha \cos\beta) \tag{3.1}$$

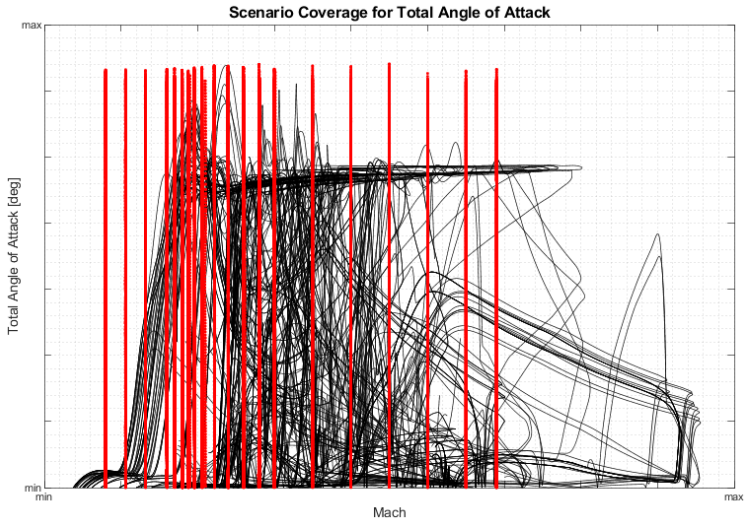

Figure 3.4: Scenario Coverage in Total Angle of Attack

3.1.1.2 Deflection Angles

3.1.1.2.1 Actual Deflections

Scenario coverage of each actual deflection angle DoE is shown in Figure 3.5. The results indicates that the fin deflection angles are covered successfully.

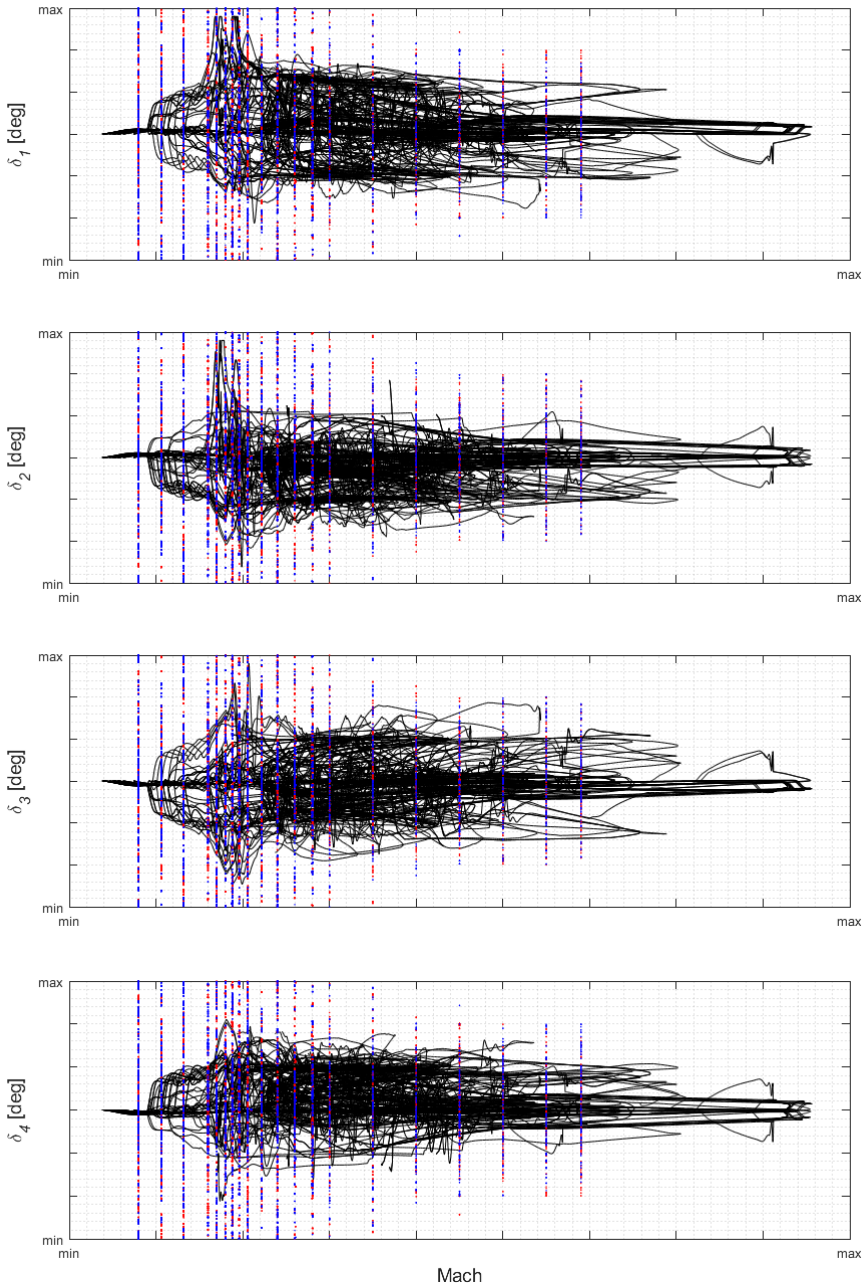

Figure 3.5: Scenario Coverage in Actual Deflections, δ_i

3.1.1.2.2 Virtual Deflections

Scenario coverage of each virtual deflection angle DoE is shown in Figure 3.6.

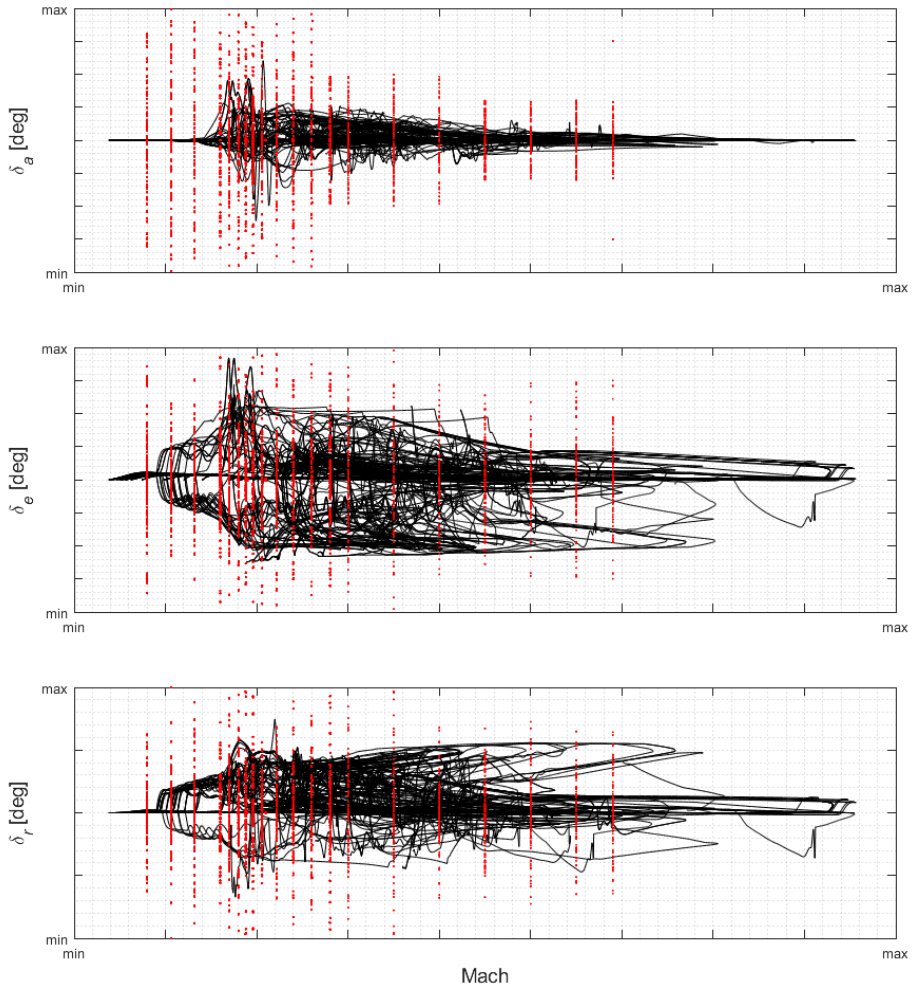

Figure 3.6: Scenario Coverage in Virtual Deflections, $\delta_{a,e,r}$

3.1.1.2.3 Cross Relations

Scenario coverage of virtual deflection cross relations of DoE are shown in the Figures 3.7-3.9.

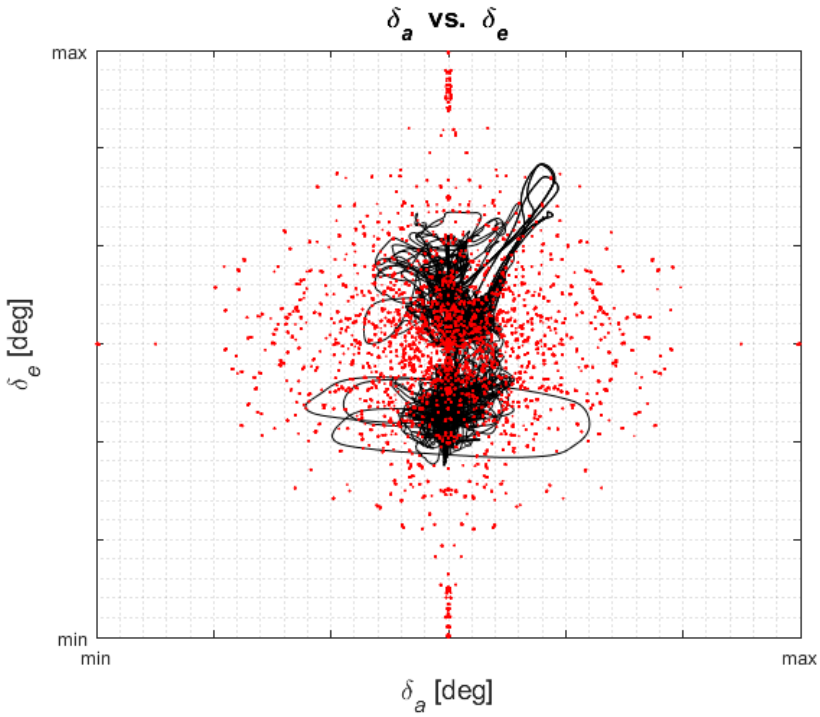

Figure 3.7: Scenario Coverage in $\delta_a - \delta_e$ Cross Relation

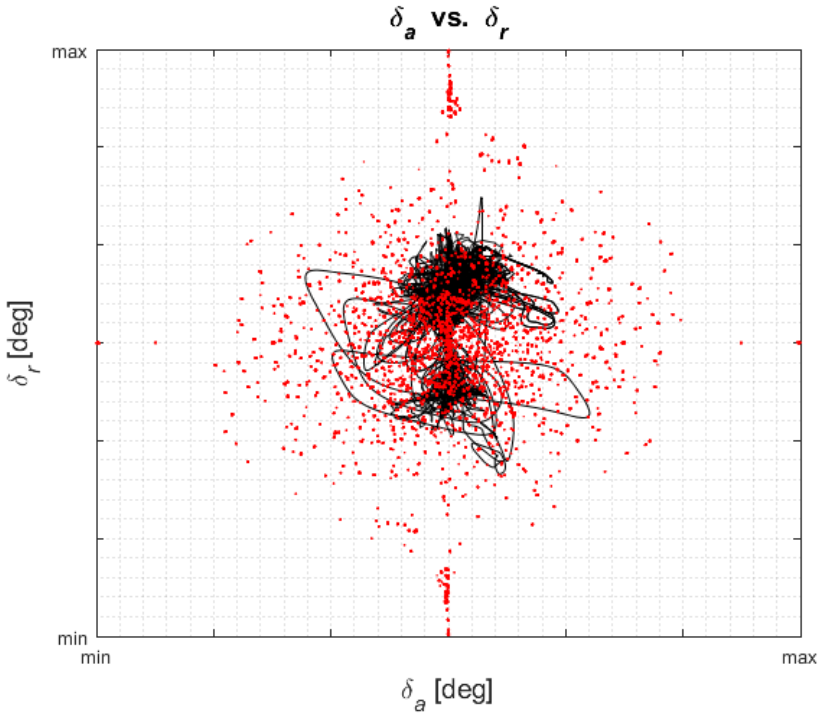

Figure 3.8: Scenario Coverage in $\delta_a - \delta_r$ Cross Relation

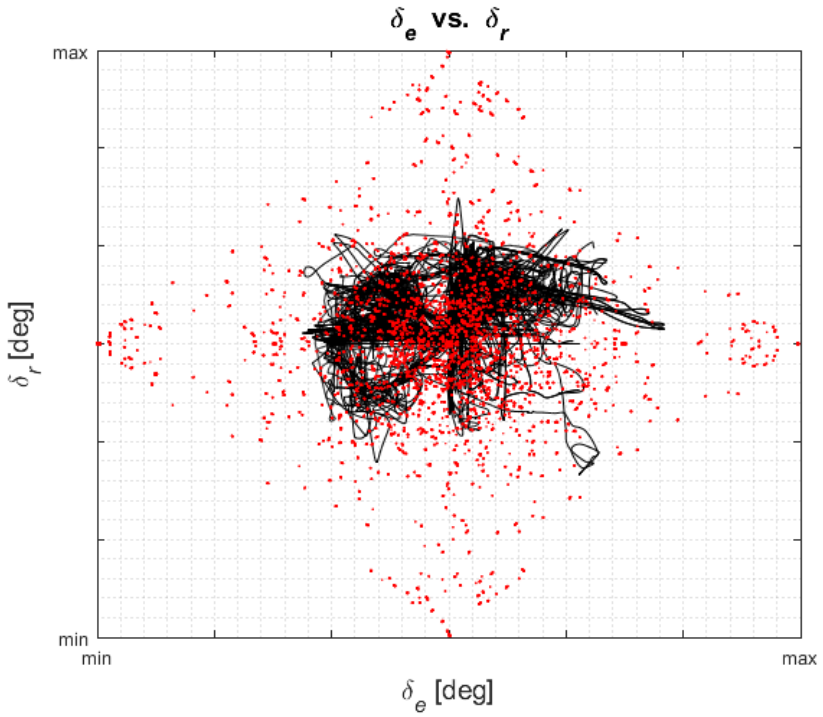

Figure 3.9: Scenario Coverage in $\delta_e - \delta_r$ Cross Relation

3.1.2 Parallel Coordinates Chart

In statistical data representation, there is a type of graph named parallel coordinates chart which is very handy when visualizing high dimensional and multivariate data.

Since the experimental design procedure is multivariate in terms of design parameters, the output can be examined using this specific chart type.

Since the chart covers all the variables and have only one y-axis, the parameters have to be either in the same scale or to be normalized. In this case, our parameters, α, β, Mach, δ_1, δ_2 , δ_3, δ_4, are not in the same scale. Therefore, the output should be normalized into a certain range.

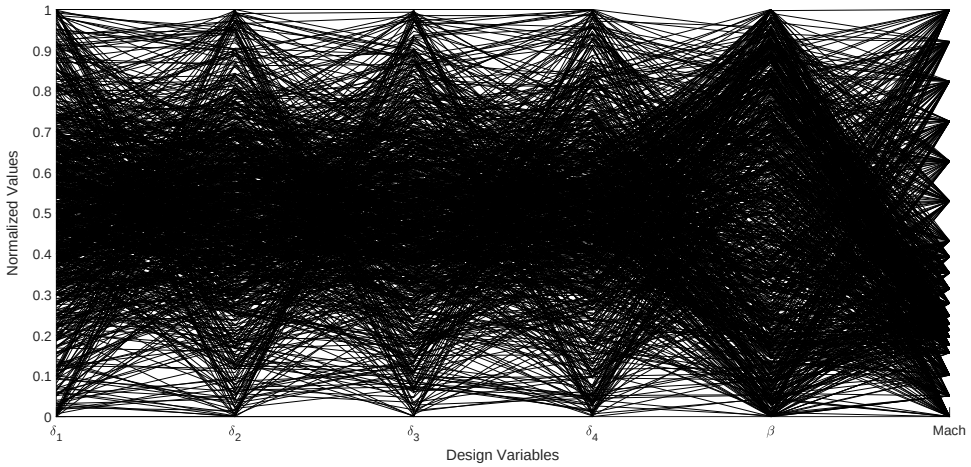

Figure 3.10: Parallel Coordinates Chart of DoE

3.2 Adaptive Downsampling Results

In Table 3.1, downsampling ratio of the aerodynamic coefficients having a relatively linear behaviour is higher, as expected. In addition, since the r^2 values are significantly high, in the applications that does not require very high accuracies, those downsampling ratios can be further decreased. By increasing the tolerance value for triangle area, with a slight data accuracy sacrifice, downsampling ratios can be further improved and the modeling speed may become faster.

Table 3.1: Downsampling Ratio for Each Coefficient

Coefficient	**Initial Size**	**Final Size**	**Downsampling Ratio**
C_x	193812	34631	17.9%
C_y	193812	23839	12.3%
C_z	193812	21046	10.9%
C_l	193812	46885	24.2%
C_m	193812	30973	16.0%
C_n	193812	32753	16.9%

Table 3.2: Downsampling Data Accuracy for Each Coefficient

Coefficient	**Minimum** r^2	**Average** r^2	**Maximum** r^2
C_x	0.995760	0.999700	1.000000
C_y	0.988430	0.999747	0.999992
C_z	0.996850	0.999921	1.000000
C_l	0.987177	0.999435	1.000000
C_m	0.996748	0.999777	0.999996
C_n	0.993106	0.999669	0.999995

In Table 3.2, downsampling accuracy of the aerodynamic coefficients having a relatively linear behaviour is higher, as expected.

Figures 3.11-3.16 shows the downsampling result for each aerodynamic coefficient.

In the upper axis, downsampling r^2 can be seen for every traverse. This value is calculated using the difference between each data point in the respective traverse. If the downsampled data represents the original test data perfectly, the value must be equal to 1. As can be seen in Table 3.2, the worst traverse of the entire test campaign appears to have $r^2 \approx 0.987$, which is more than enough for most of the applications including this one.

On the other hand, on the lower axis of each figure, there is the original versus the downsampled data graph of the traverse with the least r^2. It is drawn to make sure even the worst downsampling operation is acceptable.

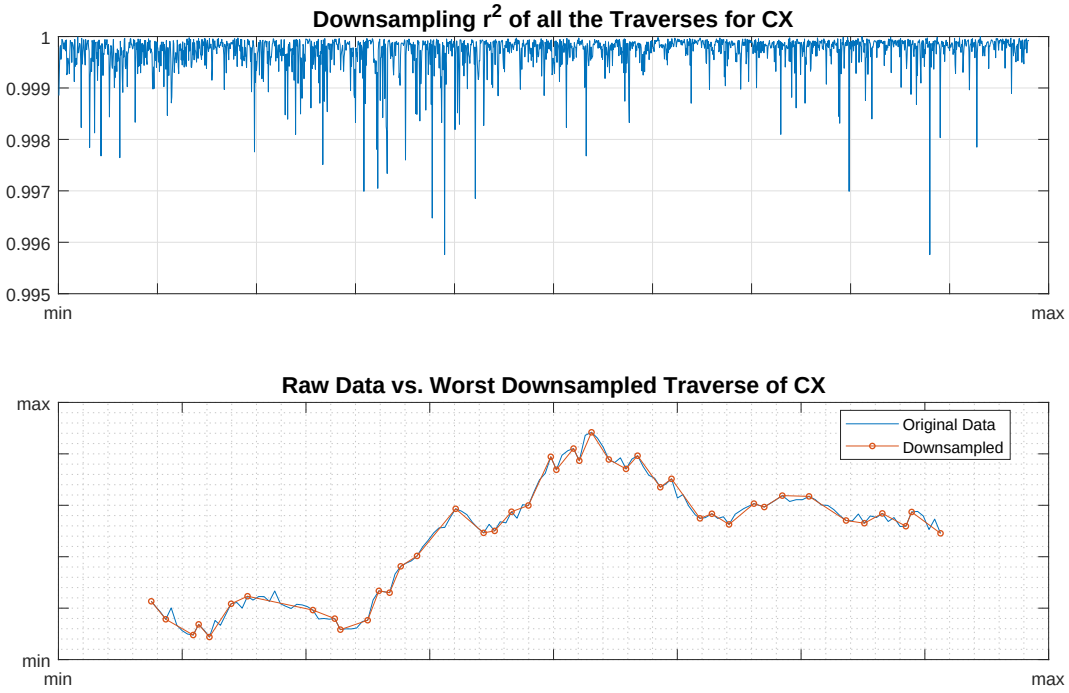

Figure 3.11: Downsampling Result for C_x

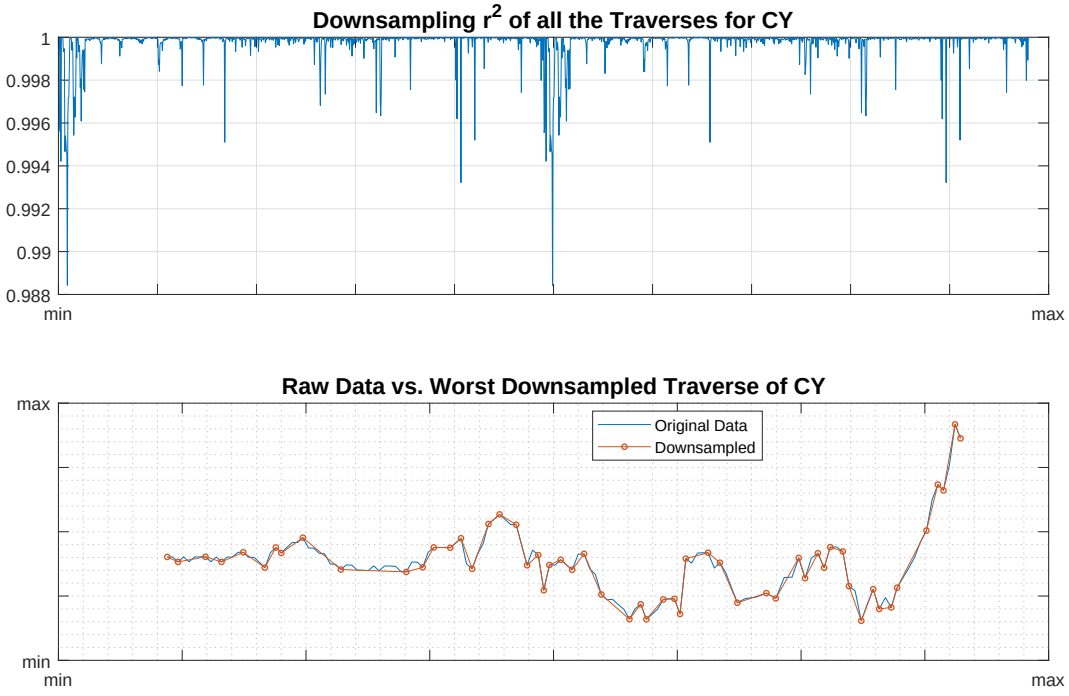

Figure 3.12: Downsampling Result for C_y

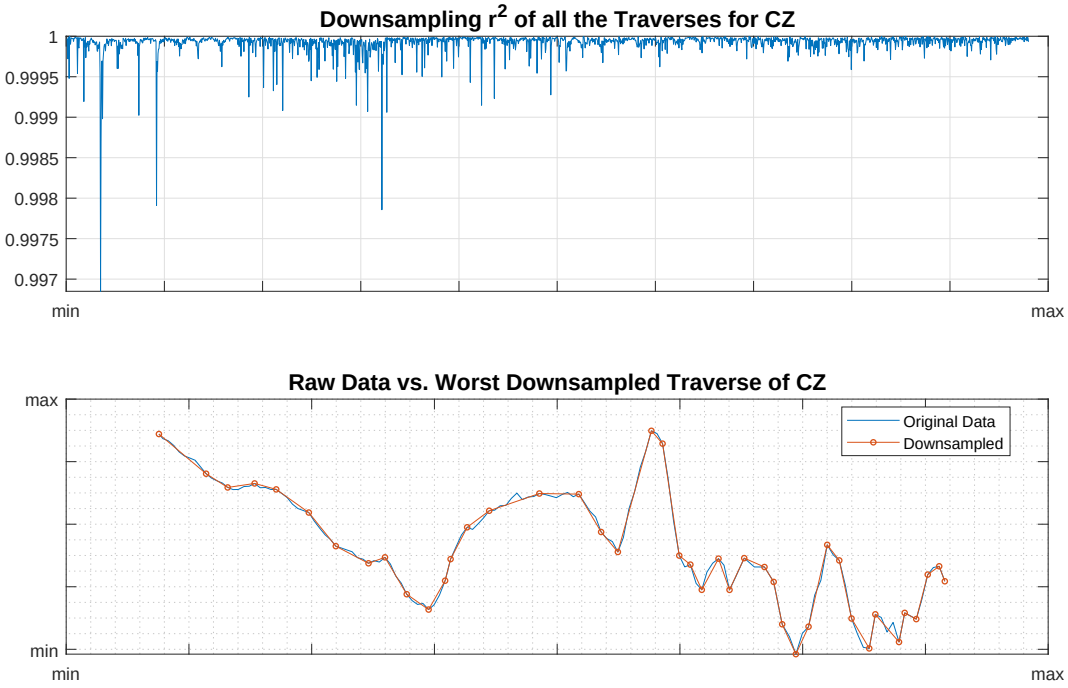

Figure 3.13: Downsampling Result for C_z

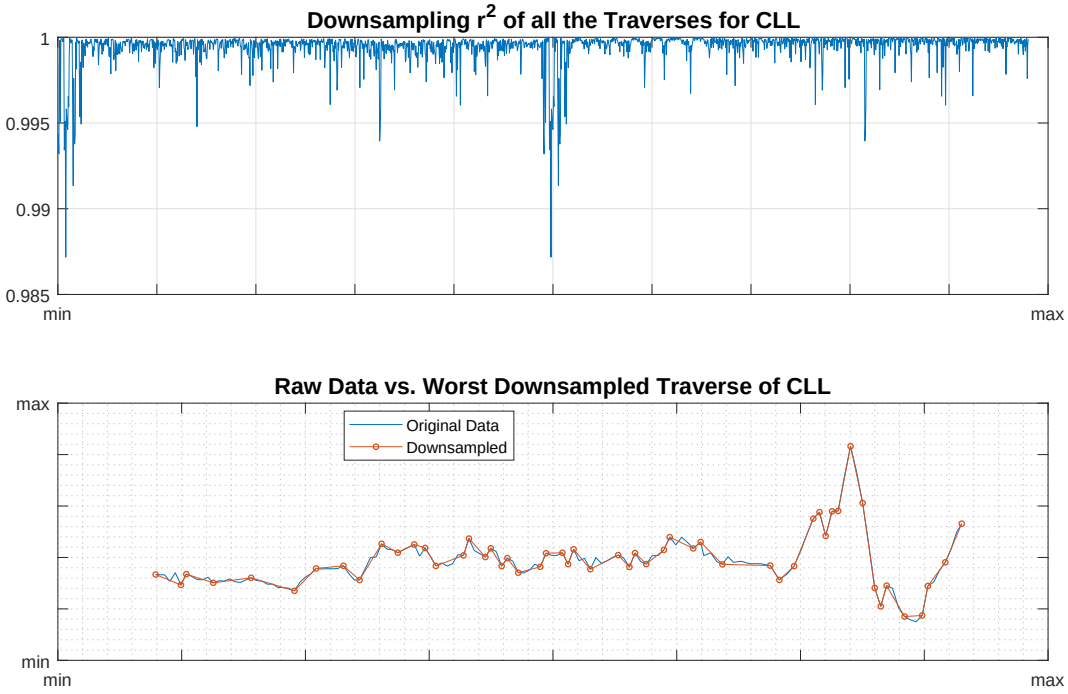

Figure 3.14: Downsampling Result for C_l

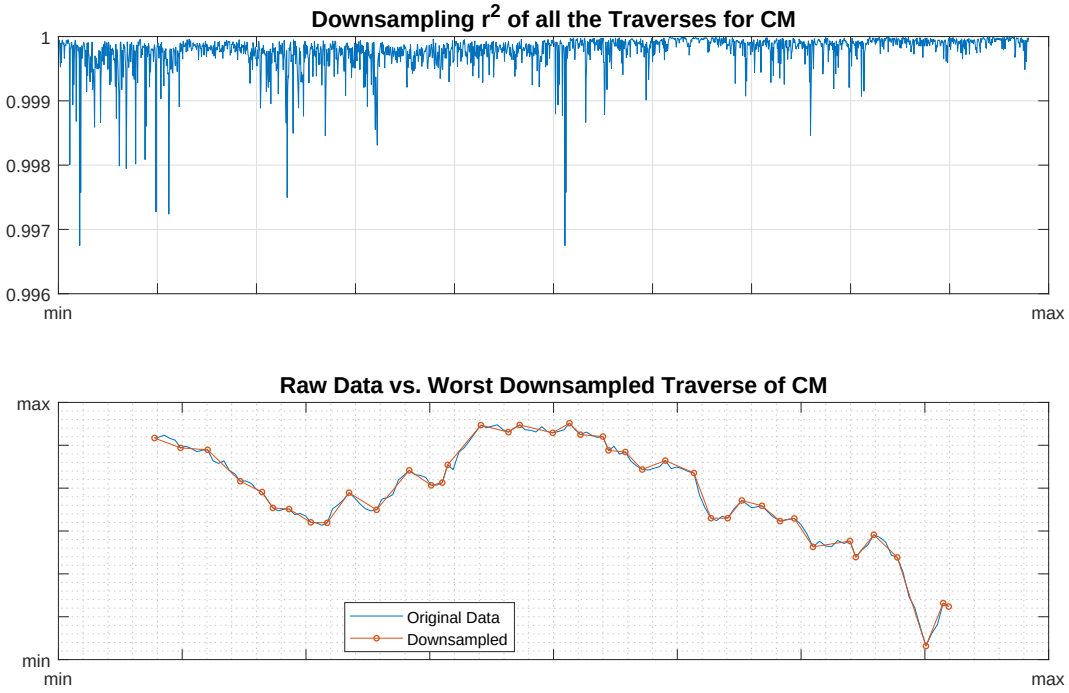

Figure 3.15: Downsampling Result for C_m

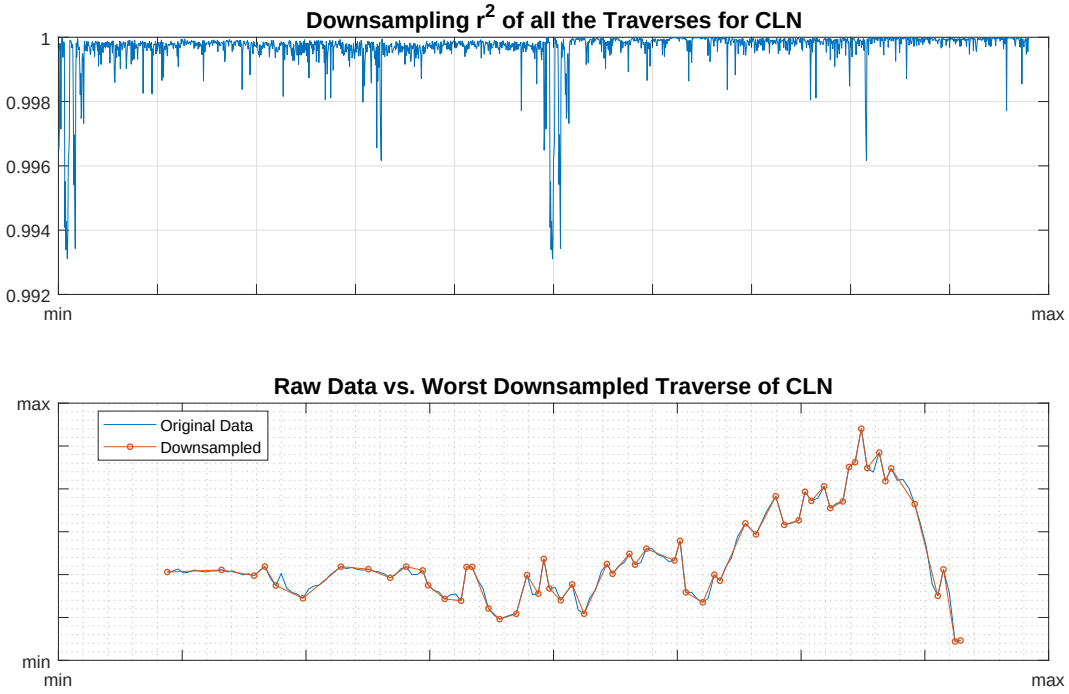

Figure 3.16: Downsampling Result for C_n

3.3 Statistical Modeling Results

In this section, modeling results are presented. Modeling results will be evaluated by their statistical performance in terms of r^2 and MSE, physical modeling performance. It is important to note that when modeling both with ANN and MARS, cross-validation is performed to see whether the test sample selection is biased or not. In this study, 5-fold cross-validation is performed and the final model is selected considering the cross-validation results.

In Figure 3.17 and Figure 3.18, random wind tunnel test results and the corresponding models that represent the same results are given. It can be seen that both ANN and MARS models cover the data well and the overfitting is not present.

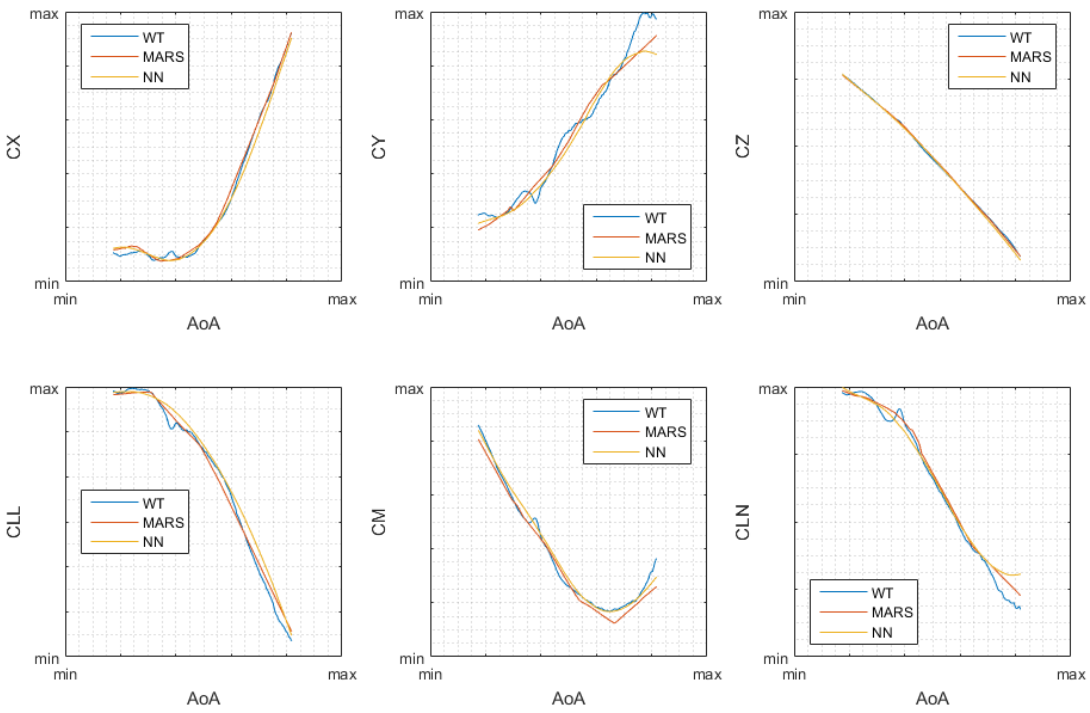

Figure 3.17: Random Test Result and Model Comparison - 1

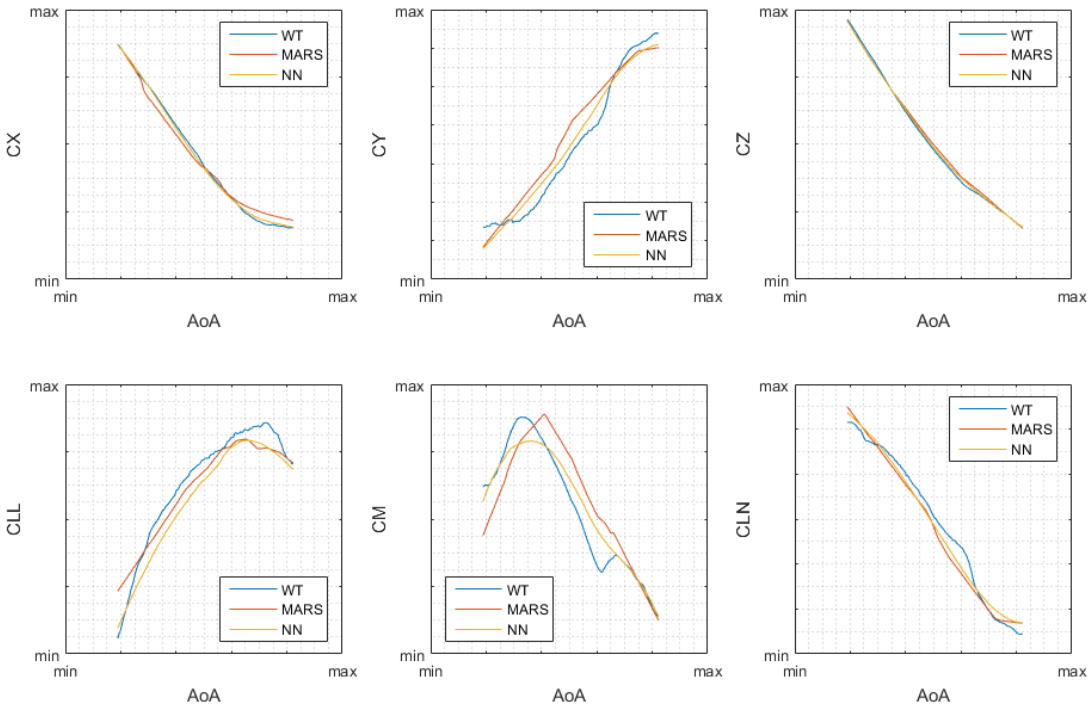

Figure 3.18: Random Test Result and Model Comparison - 2

To be able to compare ANN and MARS techniques, a pool of random points is generated within the limits of DoE. The size of the pool is above a million points which covers the space adequately. Model calculation results for each coefficient are presented in Figure 3.19.

Comparison results indicate an overall alignment of the coefficients between the techniques. Results reveal the fact that the modeling methodology of the techniques produces slightly different results for flight conditions. Considering the results for the coefficients individually, it is clear that C_y and C_z coefficients are modeled similarly by ANN and MARS techniques. On the other hand, in C_x coefficient, a widening on the shape of the resulted points, which is a sign of diverging of results, can be seen. The moment coefficients show similar behavior to the C_x coefficient. Judging by the high nonlinearity and complexity of these coefficients, it can be said that as the complexity of coefficient increases the modeling results start to differ between ANN and MARS techniques. This is an expected outcome since the functions produced

for each technique are quite different and it is not possible to dictate the success of a particular technique over the other with the information at hand. In terms of general performance, the results for MARS technique are promising considering statistical success of the technique.

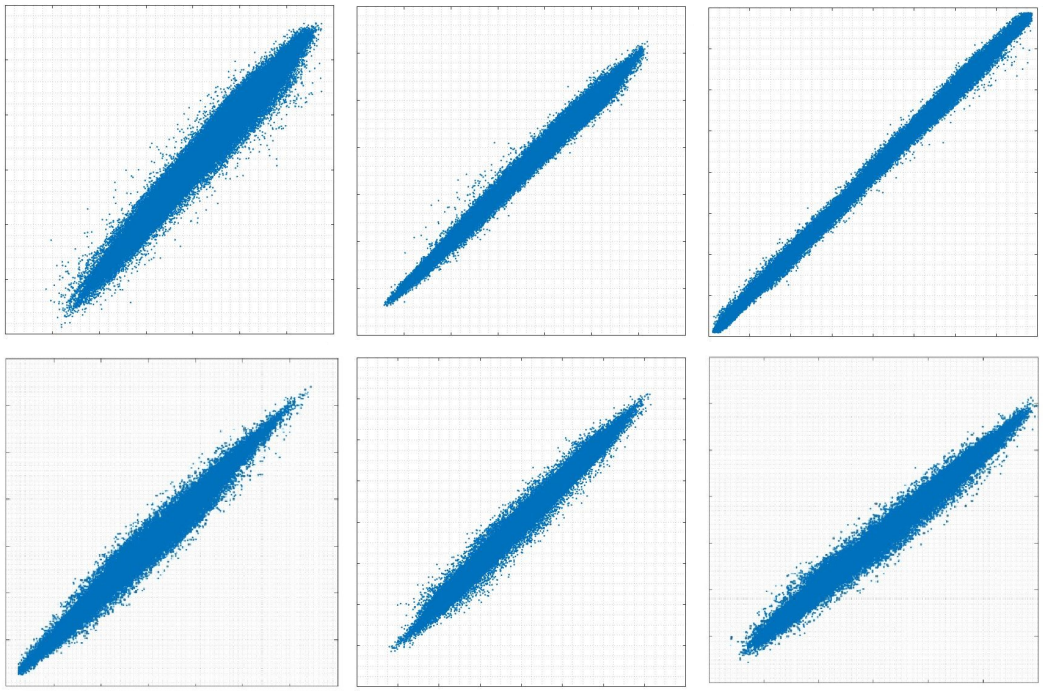

Figure 3.19: Model Correlation Table

Table 2 shows the statistical performance of each technique on every coefficient in terms of r^2 and mean squared error. According to the table, an interesting outcome is that ANN performed better in force coefficients, whereas MARS performed better in moment coefficients. Since moment coefficients are relatively more nonlinear, MARS appeared to handle the nonlinearities better.

In addition, it should be noted that r^2 is a nondimensional statistical metric, whereas MSE depends on the parameters' magnitude. Therefore, in Table 2, MSE of C_m and Cn coefficients appear to have larger values unlike the other parameters.

3.3.1 Variable Importance Check

When modeling the aerodynamic data, variable importance on each coefficient are observed and checked whether the result turns out as expected. Each parameter affects the aerodynamic coefficients in different amount. For instance, pitching moment coefficient (C_m) is mostly related with α, whereas side force coefficient (C_Y) is with β. Figure 3.20 shows the variable importance on all coefficients.

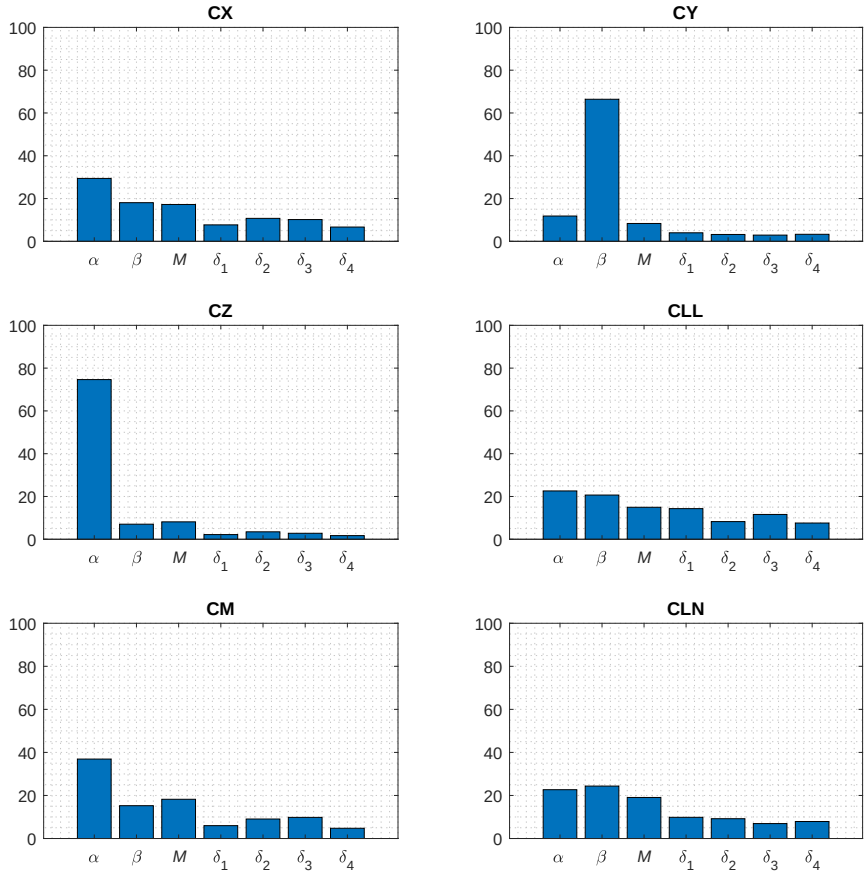

Figure 3.20: Variable Importance Check

3.3.2 Model Convergence Chart

Modeling process is not a one-step procedure. For example, when modeling with MARS, various different models are generated with changing number of basis functions. Likewise, when modeling with ANN, hidden layer size is changed and models are generated. After that, model selection is performed mainly considering statistical performance. Models are generated with increasing the number of basis functions and hidden layer size until the test sample error stops decreasing.

In Figure 3.21, statistical performances of different models of MARS and ANN are presented. As can be seen, they both converge to a value at which the r^2 reaches to its maximum and MSE reaches to its minimum. Models with larger BFs and HLSs diverge and cannot be used.

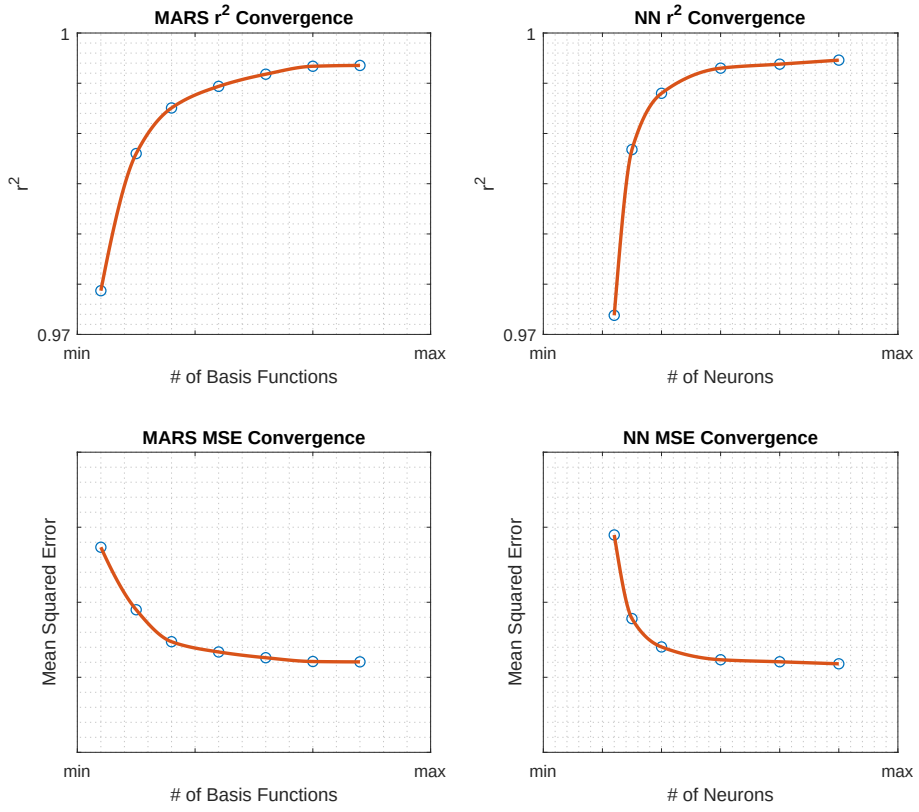

Figure 3.21: Model Convergence Comparison

3.3.3 Statistical Metrics

3.3.3.1 Coefficient of Determination

In regression analysis, there are several ways to assess the accuracy of the model or in this case goodness-of-fit. There is an important statistical metric is called the coefficient of determination and denoted as r^2.

It can be said that r^2 is related with the variance of one factor that can be caused by its relationship to another factor.

To find r^2, some other parameters are to be calculated. For the $i'th$ observation in regression, the dependent variable is denoted y_i, and its estimated value is $\hat{y}_i$. Their difference, $y_i - \hat{y}_i$ is called the $i'th$ residual.

The $i'th$ residual represents the error term when estimating the dependent variable. The sum of squares of these residuals or errors is the quantity that is minimized by the least squares method. This quantity, also known as the *sum of squares due to error*, is denoted by SSE. [14]

$$SSE = \sum (y_i - \hat{y}_i)^2 \tag{3.2}$$

SSE estimates the error through evaluating the regression mode. There is also another two parameters called SST ans SSR and they are calculated as indicated in Equation 3.3.

$$SST = \sum (y_i - \bar{y})^2 \qquad SSR = \sum (\hat{y}_i - \bar{y})^2 \tag{3.3}$$

Finally, coefficient of determination yields,

$$r^2 = \frac{SSR}{SST} = \frac{\sum (\hat{y}_i - \bar{y})^2}{\sum (y_i - \bar{y})^2} \tag{3.4}$$

Table 3.3: r_2 Comparison for Each Coefficient

r^2		
Coefficient	**MARS**	**ANN**
C_x	0.9981	0.9986
C_y	0.9985	0.9988
C_z	0.9993	0.9993
C_l	0.9907	0.9883
C_m	0.9966	0.9962
C_n	0.9945	0.9941

3.3.3.2 Mean Squared Error

Mean Squared Error (MSE) can be defined as the mean of the squared difference between the estimated values and the dependent variable itself.

Apart from r^2, MSE is dimensional, in other words, dependent on the absolute value of the data. That fact appears important while assessing the result. The analytical calculation of MSE is given in Equation 3.5.

$$MSE = \frac{SSE}{n} = \frac{1}{n}\sum(y_i - \hat{y}_i)^2 \tag{3.5}$$

where n is the number of data points

Table 3.4: MSE Comparison for Each Coefficient

MSE		
Coefficient	**MARS**	**ANN**
C_x	0.0019	0.0013
C_y	0.0309	0.0249
C_z	0.0250	0.0256
C_l	0.0229	0.0287
C_m	1.1591	1.2767
C_n	1.2423	1.3340

3.3.4 Random Input Analysis

After going through the whole modeling process and evaluating the statistical metrics, in order to test the different models random input analysis is to be performed. This is the final step before the model selection.

To do that, a large set of random input parameters has to be generated. To make a proper random input analysis, that dataset should cover as much space as possible considering the limits. In addition, it is better to test a lot of points to make sure the model performs successfully.

Following the preparation of the input dataset, those inputs are fed into the model to generate the model output for each aerodynamic coefficient.

3.3.5 Model Selection

Following procedure is performed to ensure the selection of the best model possible;

- Boundaries, limits and constraints for each design parameter are specified with prior knowledge.
- Experimental design algorithm is implemented and run many times using pre-

defined inputs.

- DoE results are thoroghly investigated using scenario coverage and parallel coordinates check.
- Selected test matrix is prepared with utmost consideration the parameter limits.
- The raw wind tunnel data is carefully acquired and pre-processed.
- Hyperparameter matrix is designed for ANN and MARS algoritmhs.
- Modeling under different hyperparameter values is monitored the results are tabulated.
- Statistical metrics such as r^2 and MSE are recorded for every run.
- 5-fold cross validation is performed for overfitting and selection bias prevention.
- Random input analysis to check whether the model complies with the parameter boundaries.
- Report generation including every coefficient model's every traverse to see the model performance in comparison to the real test data.

3.3.6 Model Integration

Following the model selection, selected model is to be integrated into 6DoF simulation model. To do that, depending on the application, there may be some post processes such as applying axial symmetry to the model, transition function implementation for the regions having risky crossings and s-function generation to increase the simulation pace.

3.4 Simulation Accuracy and Performance

The wind tunnel testing with the prepared DoE is conducted and the results are modeled with ANN and MARS techniques. Then, the aerodynamic models are integrated into a high fidelity 6DoF simulation model. Simulation results are be compared with each other in terms of flight trajectories and the specified flight parameters.

6DoF model is a large superior system that contains and unites the subsystems to be able to simulate the missile dynamics under various conditions. The objective is to simultaneously optimize the simulation accuracy and the performance. Models with higher statistical performance would lead to higher simulation accuracy, obviously. However, the model should also be able to perform faster. And, there emerges a trade-off between accuracy and performance.

3.4.1 Flight Simulations

In this section, the modeled wind tunnel test results are integrated to a high fidelity 6DoF simulation environment of the missile in order to compare ANN and MARS techniques in terms of flight parameters. For this purpose, 3 different flight scenarios which are capable of covering different Mach number, α-β and control surface deflection angle regions are determined and simulations are performed.

3.4.1.1 Scenario 1 - Non-maneuvering flight

The first scenario consists of a non-maneuvering flight, which is expected to be the most common flight scenario. One can see the difference between ANN and MARS models in Figure 3.22 in terms of trajectory, Mach, α and β.

In addition, The aerodynamic coefficients throughout the flight are shown in Figure 3.23.

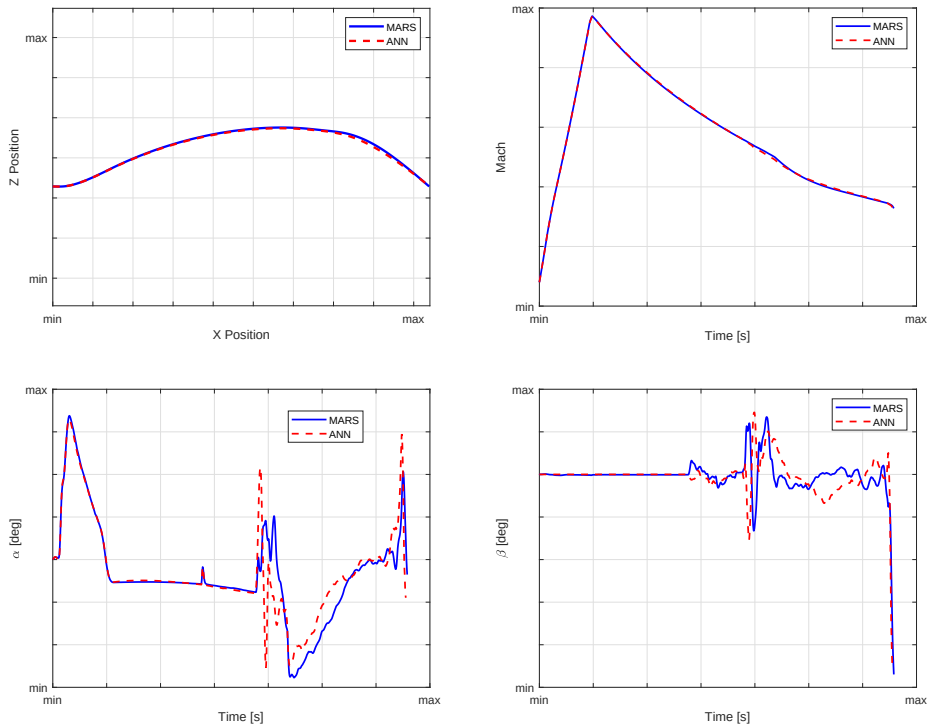

Figure 3.22: Flight Trajectory, Mach, and α and β Profiles for Scenario-1

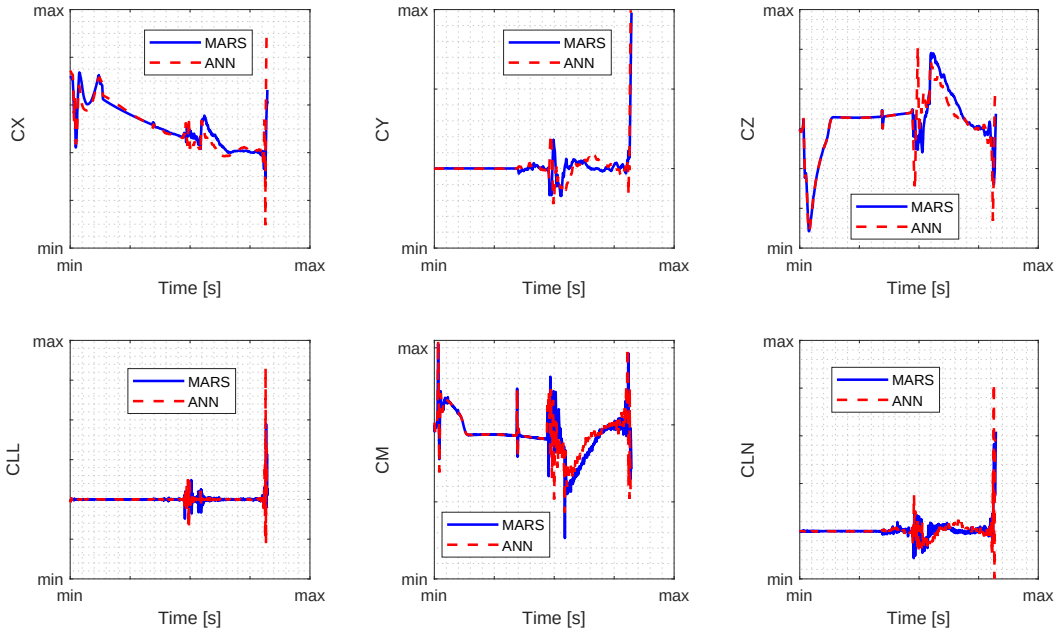

Figure 3.23: Aerodynamic Coefficients for Scenario-1

From Figure 3.22 and Figure 3.23, it can be inferred that two models behave similar in terms of trajectory and Mach number. However, there are slight differences in α and β responses and aerodynamic coefficients. Since aerodynamic coefficients and α-β values are calculated in an iterative manner, one must keep in mind that those parameters trigger each other and it is expected to see such disparities in closed loop system responses.

3.4.1.2 Scenario 2 - One Circle Maneuver

The second scenario consists of a maneuvering case in order to observe the relevant dynamic behaviour, mostly on turn performance. One can compare the effects of ANN and MARS models in Figure 3.24.

Looking in the bottom left graph, it can be seen that angles of attack have changed trends dramatically towards the end of the simulation. As the missile gets closer to the target, position estimation becomes more important and in this terminal phase, model differences yields to a target positions that are very distinct. That is why the missile requires completely different angles of attack in each simulation.

Also, the aerodynamic coefficients throughout this flight are shown in Figure 3.25.

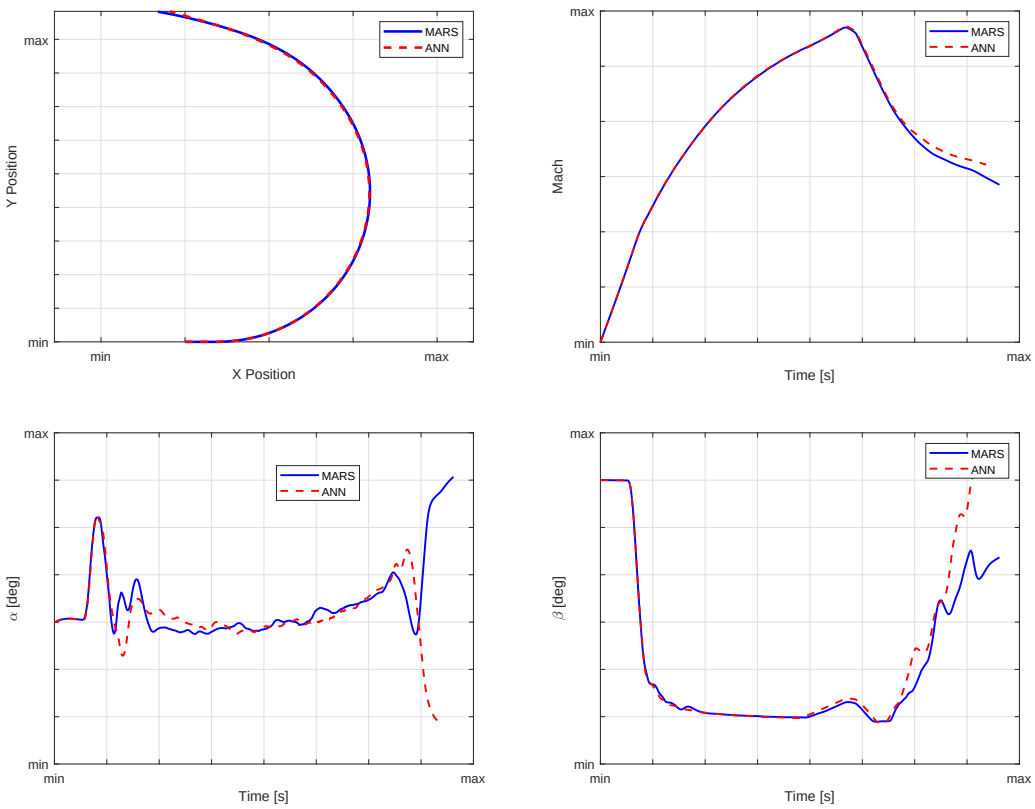

Figure 3.24: Flight Trajectory, Mach, and α and β Profiles for Scenario-2

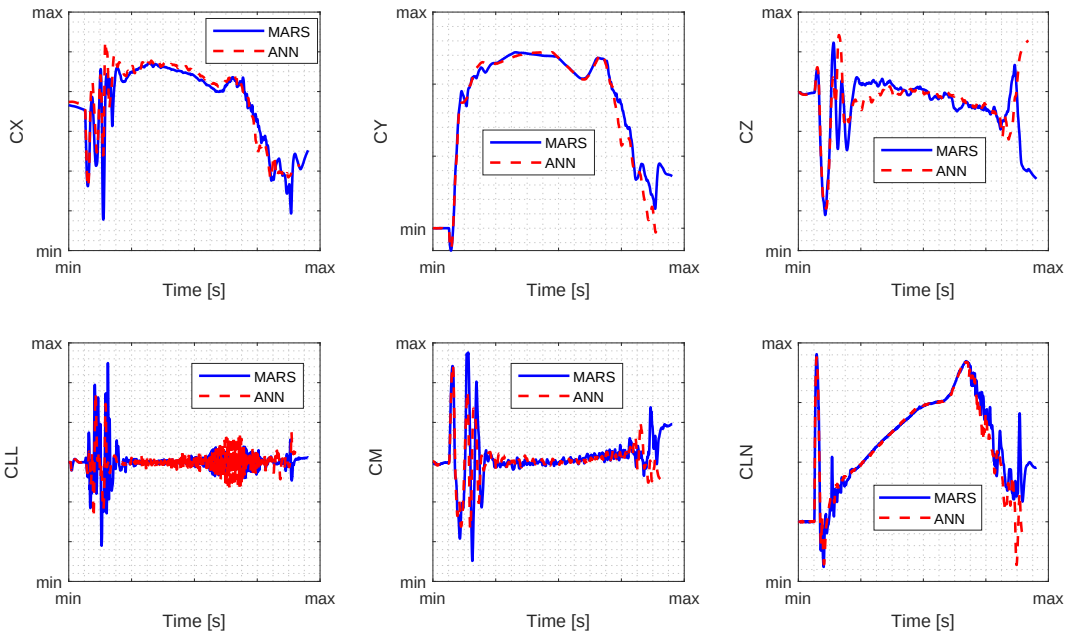

Figure 3.25: Aerodynamic Coefficients for Scenario-2

As in Scenario-1, Figure 3.24 and Figure 3.25 also show differences in aerodynamic coefficients and α and β profiles. Since this scenario focuses on β plane, the differences on C_y, C_n and β profiles appear smaller.

3.4.1.3 Scenario 3 - S-Maneuver

The third scenario is carried out under specific control surface deflections. To excite the system sufficiently and reveal various underlying dynamics, it is common practice to apply a signal that contains variety of frequencies. For this purpose, chirp signals that have magnitude 5°, duration of 15 seconds and frequency varies from 0.5 Hz to 5 Hz are applied as control surface input angles, which can be seen in Figure 3.26.

As a result of this input, rapidly changing flight conditions are expected. The resulted simulation outputs are shown in Figure 3.27.

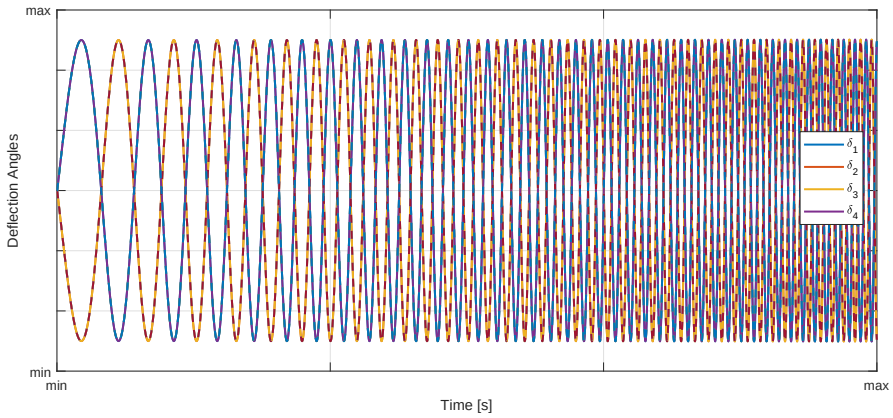

Figure 3.26: Chirp Signal Generated as Control Surface Deflections

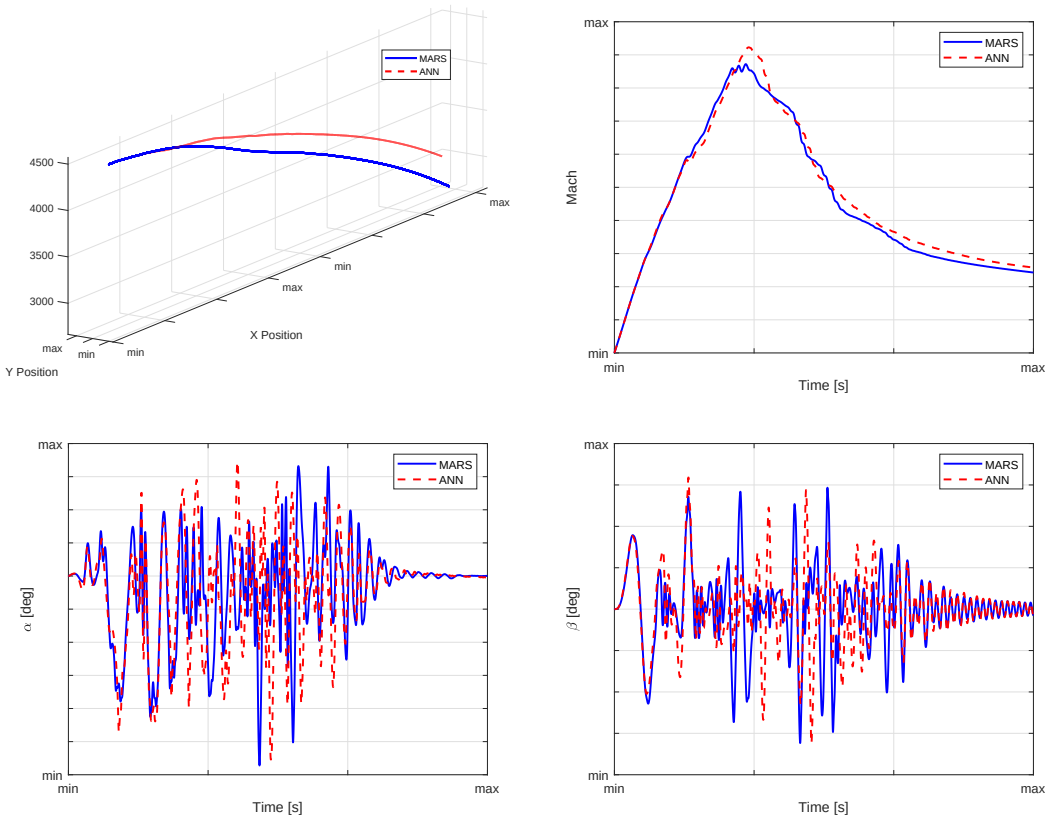

Figure 3.27: Flight Trajectory, Mach, and α and β Profiles for Scenario-3

Unlike previous scenarios, the differences in the trajectory and Mach profiles become observable. Also, the differences between α and β profiles increase as the frequency goes up. The aerodynamic coefficients throughout the flight are shown in Figure 3.28.

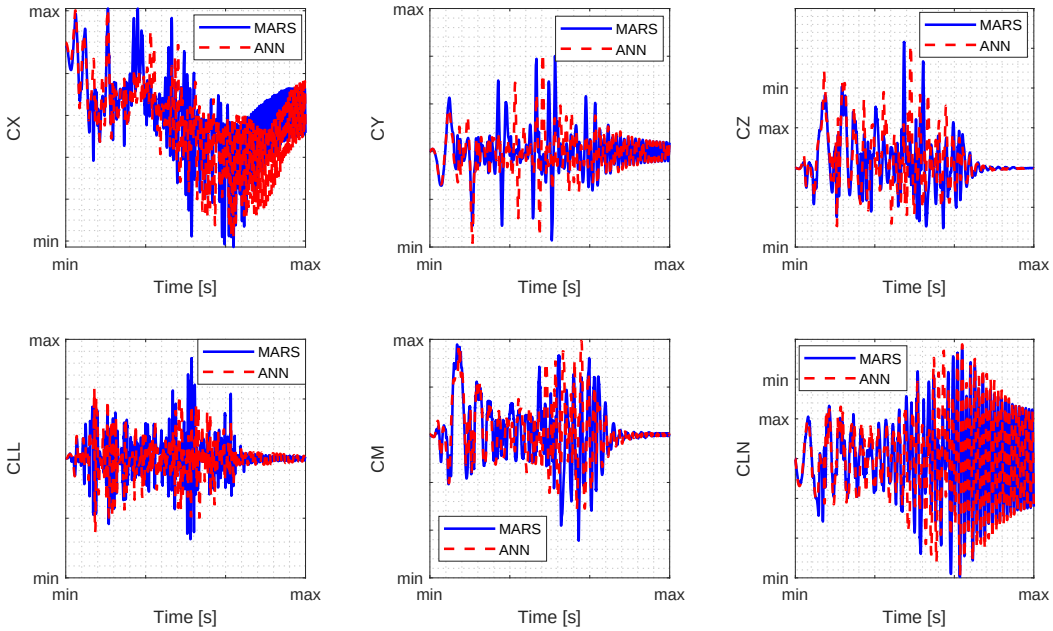

Figure 3.28: Aerodynamic Coefficients for Scenario-3

Under that challenging flight conditions, responses of aerodynamic models may provide insight about model accuracy. As the input frequency increases, the differences between two model responses become distinctive and this leads to a diversified missile trajectories and Mach profiles.

3.4.2 Simulation Runtime

In this section, various numbers of simulations are performed to see which technique is faster and consumes less computational time. All simulations are carried out in The MathWorks, Inc.'s MATLAB & Simulink and using the hardware specified below:

Table 3.5: Hardware Properties

CPU	Intel Core i5-3470 @ 3.2 GHz
Memory	8.00 GB
System Type	64-bit Operating System

In order to compare two modeling techniques in terms of simulation runtime, Simulink model (Figure 3.29) is constructed for both model functions and a batch run process is conducted for over a million uniformly distributed random inputs which are mentioned earlier in the random input analysis section. It takes ANN model to complete the simulation in 149.9 seconds whereas the MARS model's result is 128.5 seconds. Consequently, using ANN instead of MARS costs approximately 17% more computational time.

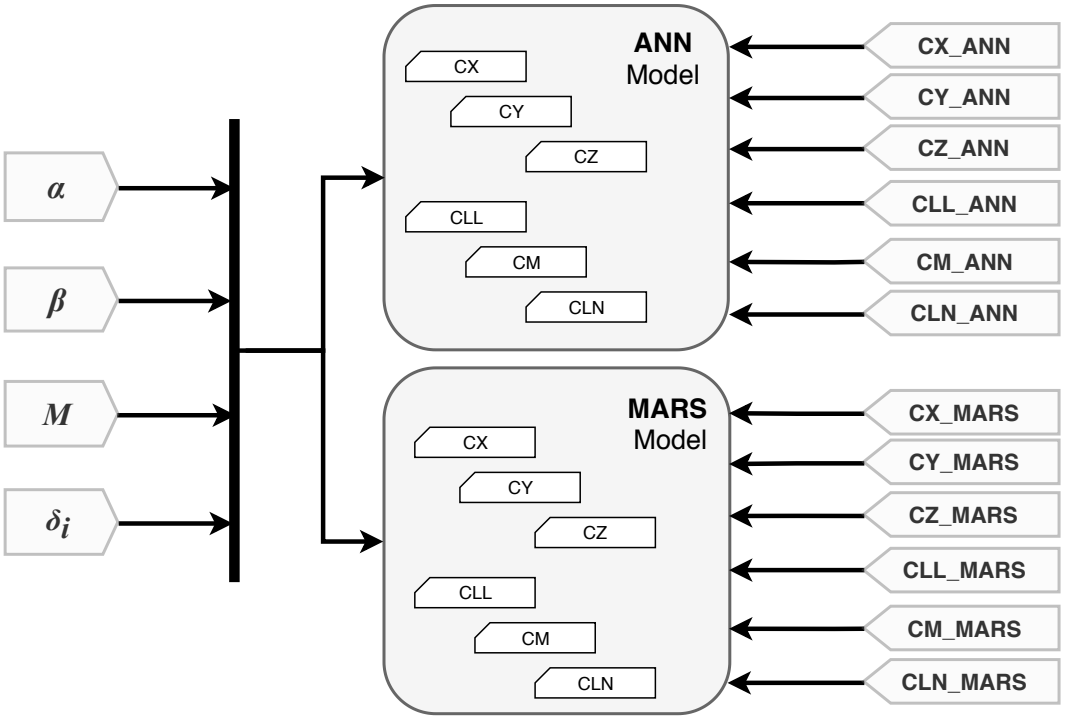

Figure 3.29: Batch Run Model for Simulation Performance Assessment

CHAPTER 4

CONCLUSION

In this thesis, a methodology for experimental design for wind tunnel testing and modeling of the collected aerodynamic data for an agile missile is presented. The ultimate aim is to improve the 6DoF simulation accuracy and performance by better representation of the aerodynamics.

Wind tunnel tests are quite necessary when evaluating the aerodynamics of air vehicles. However, since testing is also costly, the process should be optimized to obtain the maximum benefit. In most cases, all the design space cannot be tested due to time and cost concerns. Therefore, DoE is considered to determine the test matrix. DoE is a vast subject in statistics and there are lots of different algorithms. Among those different algorithms, sequential space filling is selected when designing the experiment. Because, wind tunnel tests mostly conducted in several phases and sequential space filling is well suited for this kind of procedure.

Due to highly nonlinear nature of the aerodynamic properties of an agile missile, nonparametric modeling tools are considered to model the output of the wind tunnel test. ANN modeling technique, which is in common use in the field, is utilized to construct models to predict aerodynamic coefficients during simulations. MARS technique is also utilized as a new tool to model the wind tunnel data for its consideration as a contender to ANN technique.

Both techniques are found to be successful in modeling of the aerodynamic coefficients. The statistical modeling performance of MARS is similar to that of ANN. However, MARS appeared to have better statistical performance on moment coefficients which usually have more nonlinear behavior compared to the force coefficients.

After the modeling is completed, aerodynamic models are integrated into 6DoF equations of motion model in order to assess their accuracy and performance. In flight simulations, both techniques perform closely under 3 different scenarios. Yet, the difference between the techniques becomes more observable as the scenario covers broader flight regime. Batch run study tells that MARS appeared 17% faster in terms of computational time. As a result, both techniques appeared to be well suited for the solution of the problem with minor differences when applied in correct manner.

Consequently, it can be said that the methodology given in this thesis is quite meaningful and yields to a good result. Aerodynamic modeling of the agile missile that has a large flight envelope with a limited budget can be considered a big challenge. Nevertheless, when performed correctly, experimental design and nonlinear statistical modeling is proven to be successful when overcoming that complex problem.

4.1 Future Works

- Improvements on hyperparameter tuning procedure, e.g automation
- Test matrix updates and interruptions with on-site modeling
- Transfer learning application using system identified flight test data

REFERENCES

[1] AMRAAM Missile 3D Model. https://www.3dcadbrowser.com/3d-model/amraam-missile. [Online; accessed 04-April-2019].

[2] Vladislav Klein and Eugene A. Morelli. *Aircraft System Identification: Theory and Practice*. American Institute of Aeronautics and Astronautics, 2006.

[3] Michael Cook. *Flight Dynamics Principles: A Linear Systems Approach to Aircraft Stability and Control*. Elsevier Aerospace Engineering Series, USA, 2007.

[4] U. Kutluay. Fin Mixing Optimization to Minimize Control Coupling Effects. In *Ankara International Aerospace Conference (AIAC 2013)*, 2013.

[5] O. Savas, E. Topbas, K. Unal, H. D. Karaca, and A. T. Kutay. Experimental Design and Statistical Modelling Methodology for Wind Tunnel Aerodynamics of an Agile Missile to Improve the Simulation Accuracy and Performance. In *AIAA Modeling and Simulation Technologies Conference*, 2018.

[6] R. DeLoach. Applications of Modern Experiment Design to Wind Tunnel Testing at NASA Langley Research Center. In *36th AIAA Aerospace Sciences Meeting and Exhibit*, 1998.

[7] C. F. Lo, J. L. Zhao, and R. DeLoach. Application of Neural Networks to Wind Tunnel Data Response Surface Methods. In *AIAA Aerodynamic Measurement Technology and Ground Testing Conference*, 2000.

[8] K. Crombecq, I. Couckuyt, D. Gorissen, and T. Dhaene. Space-Filling Sequential Design Strategies for Adaptive Surrogate Modelling. In *International Conference on Soft Computing Technology in Civil, Structural and Environmental Engineering*, 2009.

[9] K. Crombecq and T. Dhaene. Generating Sequential Space-Filling Designs Us-

ing Genetic Algorithms and Monte Carlo Methods. In *Asia-Pacific Conference on Simulated Evolution and Learning (SEAL 2010)*, 2010.

[10] S. T. Selvi, S. Rama, and E. Mahendran. Neural Network based Interpolation of Wind Tunnel Test Data. In *International Conference on Computational Intelligence and Multimedia Applications (ICCIMA 2007)*, 2007.

[11] Patel Nitin. *15.062 Data Mining*. Massachusetts Institute of Technology: MIT OpenCourseWare, https://ocw.mit.edu. License: Creative Commons BY-NC-SA, Spring 2003.

[12] Jerome H. Friedman. Multivariate Adaptive Regression Splines. *The Annals of Statistics , Vol . 19 , No . 1*, March 1991.

[13] Trevor Hastie, Robert Tibshirani, and Jerome Friedman. *The Elements of Statistical Learning: Data Mining, Inference and Prediction*. Springer, August 2008.

[14] David R. Anderson, Dennis J. Sweeney, and Williams Thomas A. *Statistics for Business and Economics*. Thomson South-Western, 2008.